

The space photometry revolution

**Partie deux:
Extrasolar planets and planetary systems**



July 6 – 11, 2014 – Toulouse, FRANCE

R. Gilliland: Why a revolution?

CoRoT launched: 27.XII.2006

Kepler launched: 7.III.2009



Discoveries	< 1994	1999	2004	2009	2014
Exoplanets	4	25	120	265	1 382
Asteroseismology	0	0	10	380	15 000+

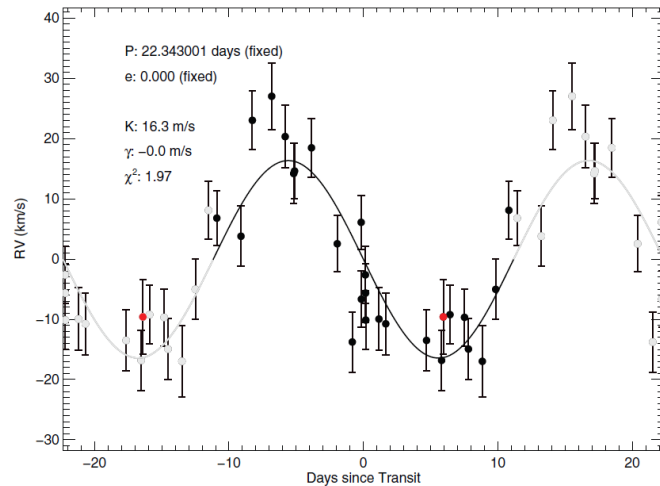
K2: III.2014

TESS: 2017 (Transiting Exoplanet Survey Satellite)

PLATO: 2024 (PLANetary Transits and Oscillation of stars)

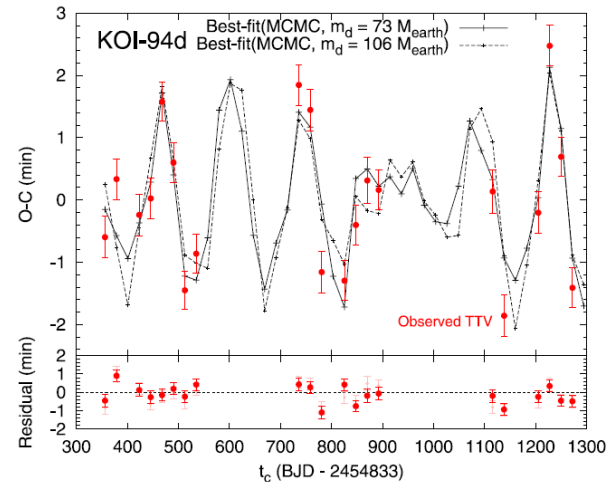
A. Santerne: From super-Earths to brown dwarfs

M determination: RV, TTV... (e.g. KOI-94d)



$$m_d = 106 \pm 11 M_{\oplus}$$

(Weiss et al., 2013: *ApJ*, **768**, 14)



$$m_d = 52.1^{+6.9}_{-7.1} M_{\oplus}$$

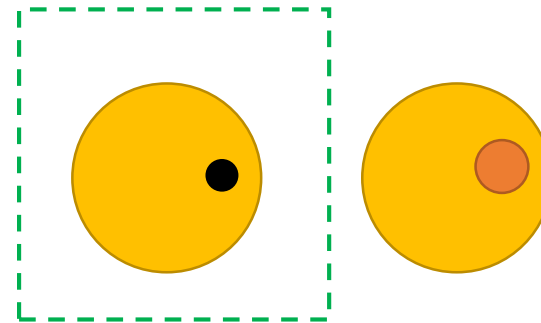
(Masuda et al., 2013: *ApJ*, **778**, 185)

A. Santerne: From super-Earths to brown dwarfs

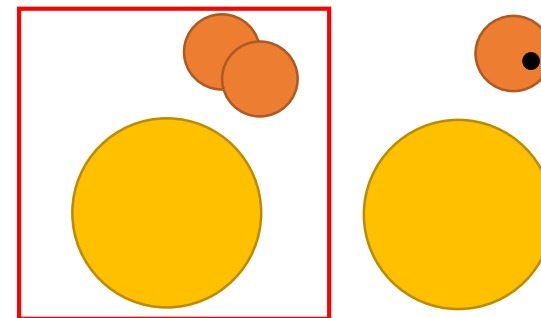
M determination: RV, TTV...

False positive signals:

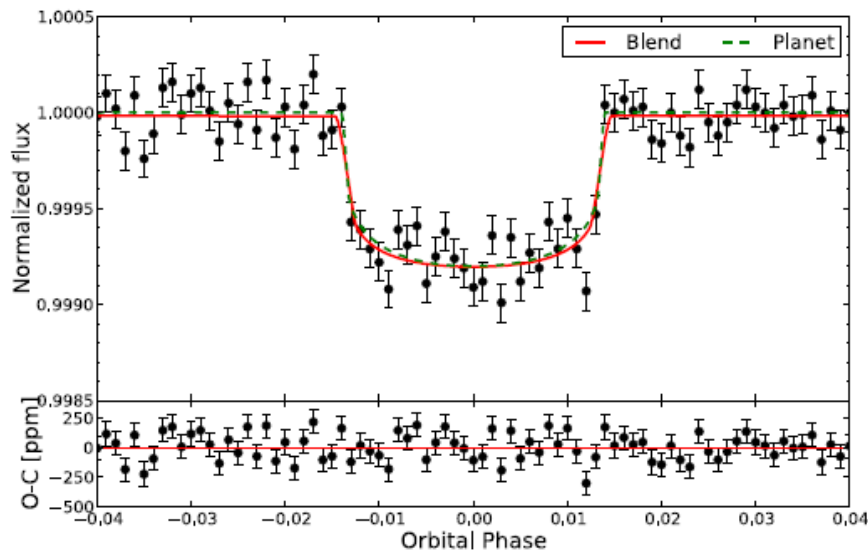
- Stellar blend



Radius estimation error



(Cameron, 2012: *Nature*, **492**, 48)

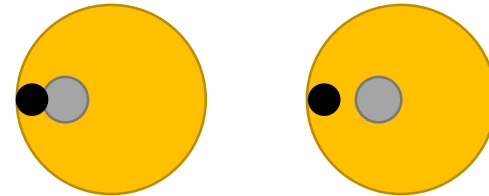


A. Santerne: From super-Earths to brown dwarfs

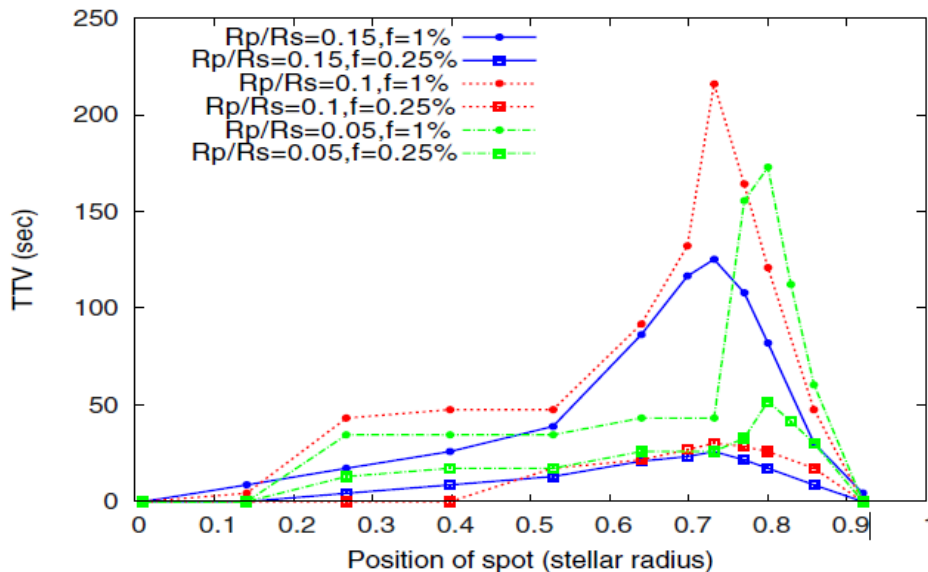
M determination: RV, TTV...

False positive signals:

- Stellar blend
- Planet/spot occultation



Fake TTV/TDV



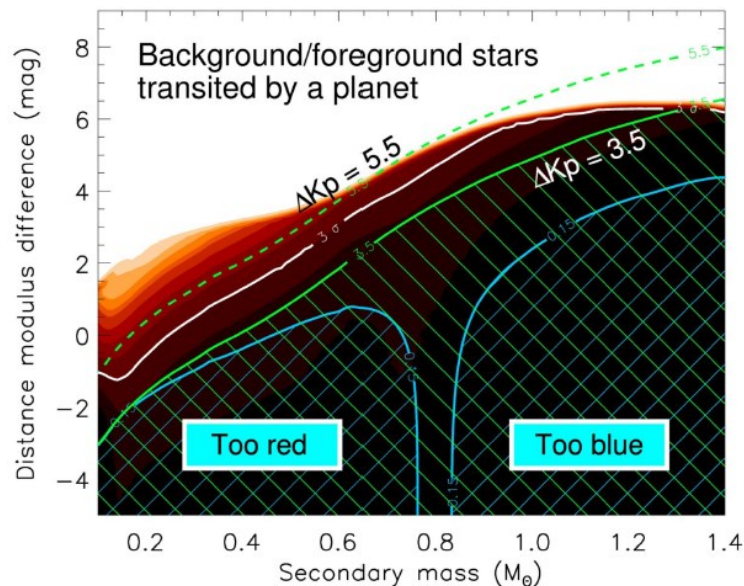
(Oshagh et al., 2013: *A&A*, 556, 19)

A. Santerne: From super-Earths to brown dwarfs

Planetary statistics needs (census 2014):

- Accurate false positive determination
- Better pipelines (instrumental profile reduction)
- More objects (hot Jupiters from Kepler, neptunes from CoRoT – bias?)
- Better R_{\star} to compute better R_p

BLENDER – planetary transit validation (Torres et al., 2011: *ApJ*, **727**, 24)



A. Santerne: From super-Earths to brown dwarfs

Planetary statistics needs (census 2014):

- Accurate false positive determination
- Better pipelines (instrumental profile reduction)
- More objects (hot Jupiters from Kepler, neptunes from CoRoT – bias?)
- Better R_{\star} to compute better R_p

PASTIS (Planetary Analysis and Small Transit Investigation Software)

- Models LC and follow-up obs., validation of planet parameters

Stellar Parameters

T_{eff}	Effective temperature
z	Stellar atmospheric metallicity
g	Surface gravity
M_{init}	Zero-age main sequence mass
τ_{\star}	Stellar age
ρ_{\star}	Bulk stellar density
$v \sin i_{\star}$	projected stellar rotational velocity
ua, ub	Quadratic-law limb darkening coefficients
β	Gravity darkening coefficient
d	Distance to host star

Planet Parameters

M_p	Mass
R_p	Radius
albedo	Geometric Albedo

System Parameters

k_r	secondary-to-primary (or planet-to-star) radius ratio, R_2/R_1
a_R	semi-major axis of the orbit, normalized to the radius of the primary (host) star, a/R_1
q	mass ratio, M_2/M_1

Orbital Parameters

P	orbital period
T_p	time of passage through the periastron
T_c	time of inferior conjunction
e	orbital the eccentricity
ω	argument of periastron
i	orbital inclination
v_0	center-of-mass radial velocity

A. Santerne: From super-Earths to brown dwarfs

Planetary statistics needs (census 2014):

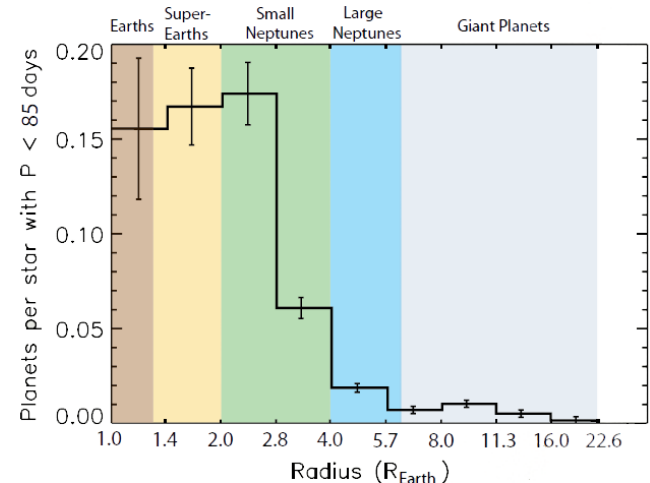
- Accurate false positive determination
- Better pipelines (instrumental profile reduction)
- More objects (hot Jupiters from Kepler, neptunes from CoRoT – bias?)
- Better R_{\star} to compute better R_P

PASTIS (Planetary Analysis and Small Transit Investigation Software)

- Models LC and follow-up obs., validation of planet parameters

Statistics:

- 22 ± 8 % of sun-like stars with earth-size planet in their HZ
- 15^{+13}_{-6} % of Kepler objects have 2 earth-size planet in their HZ



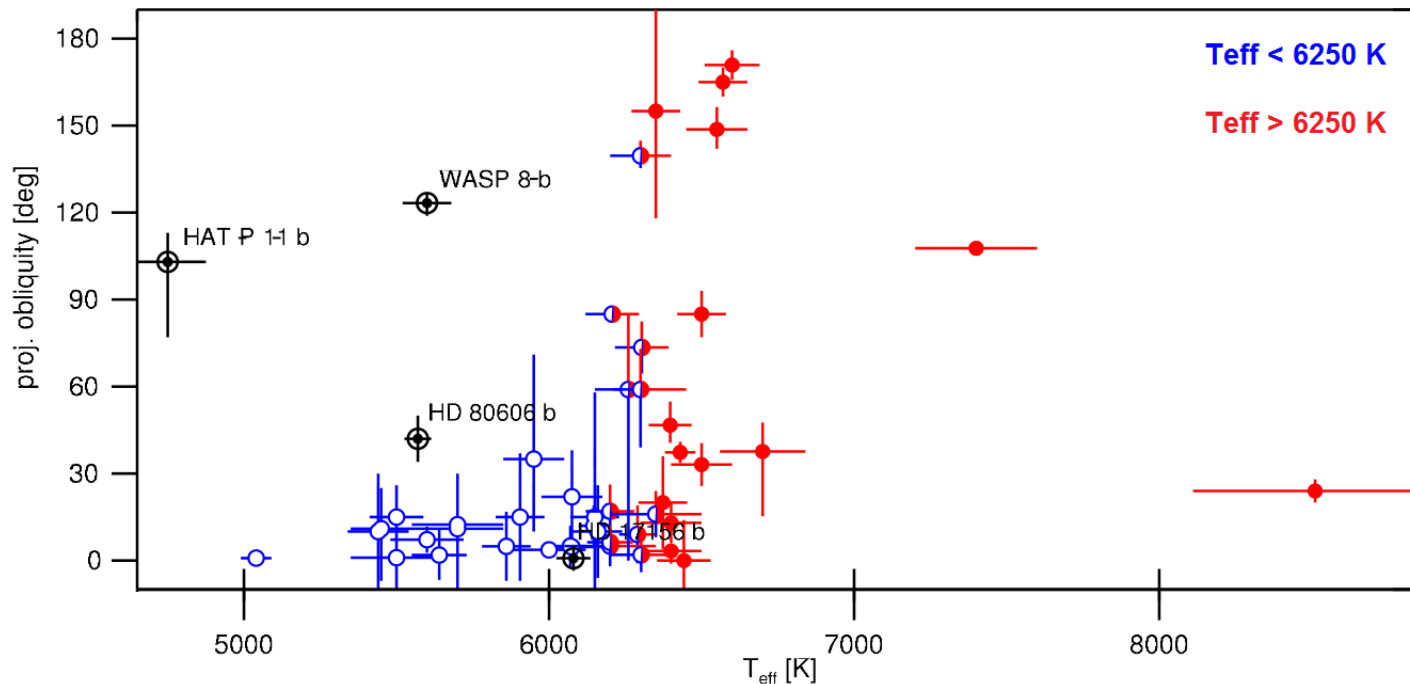
(Fressin et al., 2013: *ApJ*, **766**, 81)

D. Gandolfi: CoRoT-32b – youngest aligned exoplanet

Planet migration theory changes a , e (Aligned systems)

Kozai mechanism changes a , e , i (Misaligned systems)

Tides are more efficient @ cold stars (with convective zone)



(Albrecht et al., 2012: *ApJ*, **757**, 18)

D. Gandolfi:

CoRoT-32b – youngest aligned exoplanet

Star: F4V ($T_{\text{eff}} = 6670$ K), $P_{\text{rot}} = 0.81$ d (from stellar activity)

Observed RM effect – orbital & rot axis ($\lambda = 0.4^\circ$)

Li-rich star (Li is more depleted in colder stars) => age 15-30 Myr

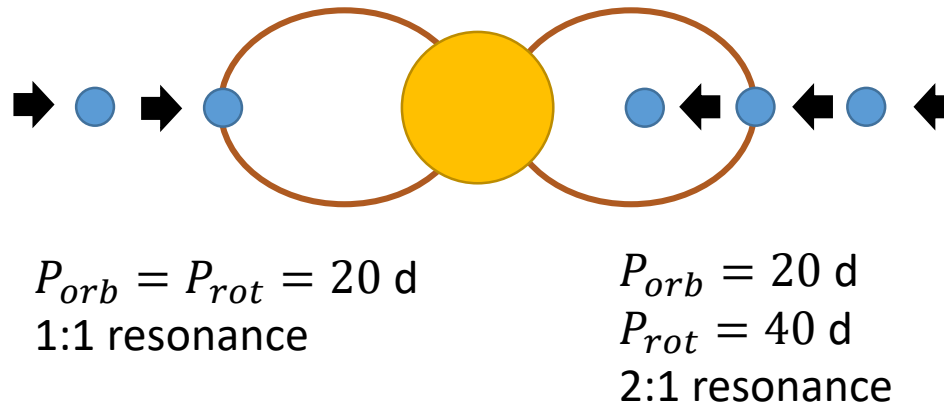
Star member of NGC 2232 (25 Myr – old cluster)

Planet $v \sin i = 0$ @ transit mid point → aligned in the line-of-sight

Alignment timescale > 100 Gyr → primordial alignment?

D. Gandolfi: CoRoT-32b – youngest aligned exoplanet

Two scenarios of hot Jupiter migration:



Young system – L cannot be lost through winds

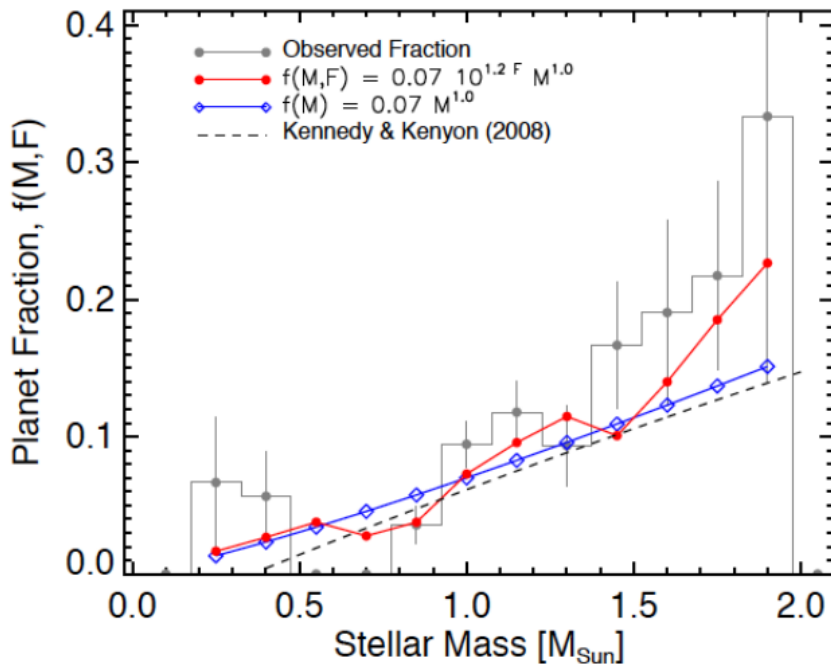
Evolutionary track for the star to find at least 1:1 resonance: **0.6 Myr**

E. Günther: CoRoT-35b – polar orbit planet

Primordial disk lifetime @ hot stars is shorter

$$M_{\star} \sim 1M_{\odot}: \tau_{disk} = 2.5 \text{ Myr} \quad M_{\star} \sim 1.3M_{\odot}: \tau_{disk} = 1.2 \text{ Myr}$$

CoRoT detection limits: $1 R_J$ (B-stars) and $2 R_E$ (G-stars)



(Johnson et al., 2010: *PASP*, **122**, 894)

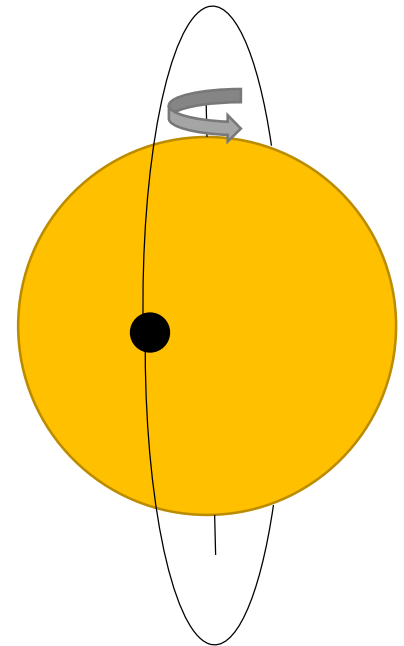
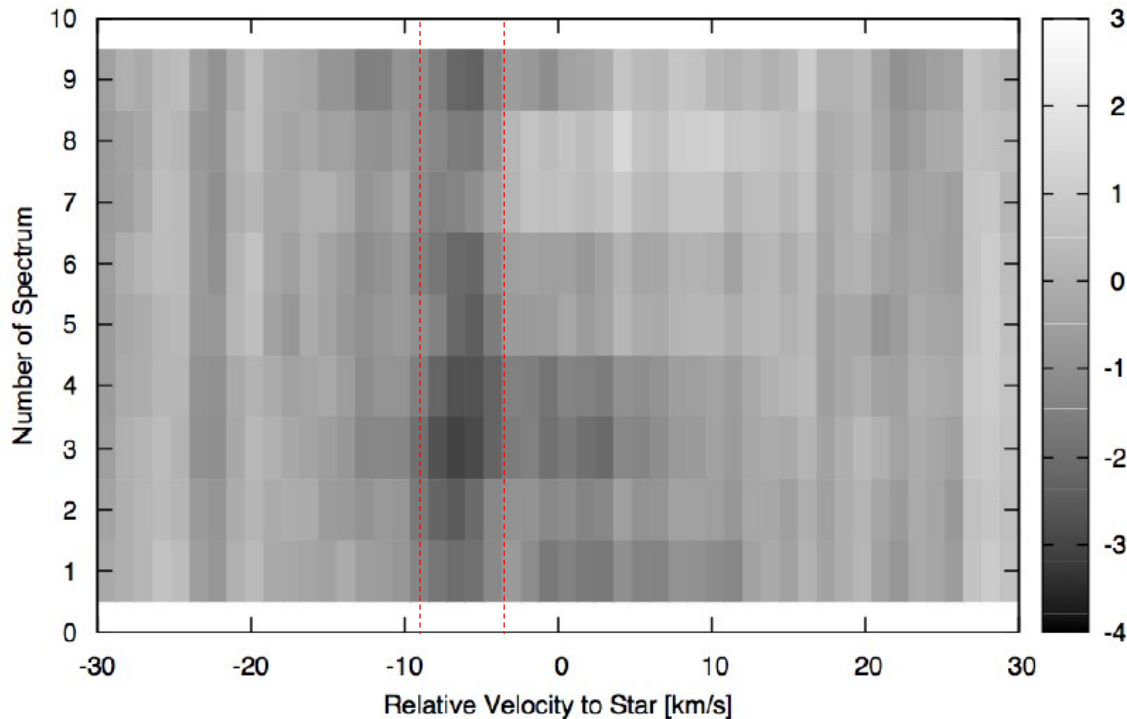
Sp. type	% planets	CoRoT sample	M_{\odot}
A	0 - 5%	16%	1.3 - 3.2
F	30 - 32%	35%	1.1 - 1.3
G	50 - 54%	15%	0.9 - 1.1
K	13 - 16%	5%	0.4 - 0.8

E. Günther: CoRoT-35b – polar orbit planet

Follow-up: Hi-res spectroscopy, AO imaging

$$P_{\text{orb}} = 5.6 \text{ d}, M_{\star} = 1.4 M_{\odot}, R_P = 1.9 R_J$$

Observed RM effect \rightarrow polar orbit? (check for surface features of \star)

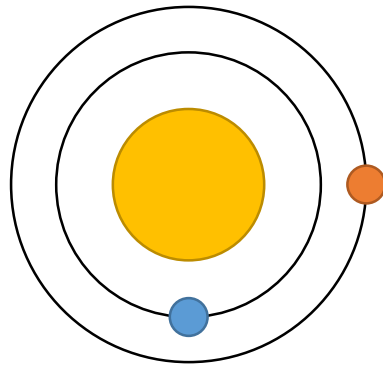


A. Ofir: TTV in Kepler data

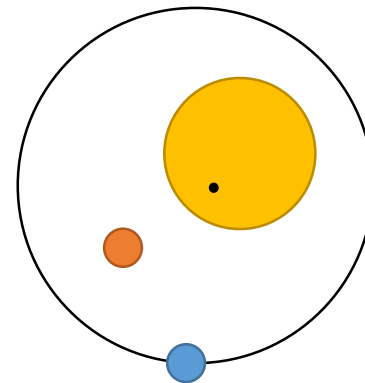
TTV caused:

- angular momentum exchange between planets (direct)
- host star moves around barycentrum (indirect)

First observed: 2010 – Kepler-9 (Holman et al., 2010: *Science*, **330**, 51)



(Holman & Murray, 2005:
Science, **307**, 1288)

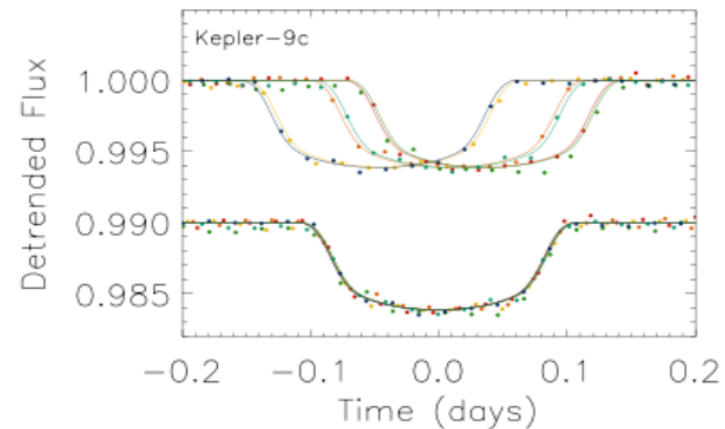
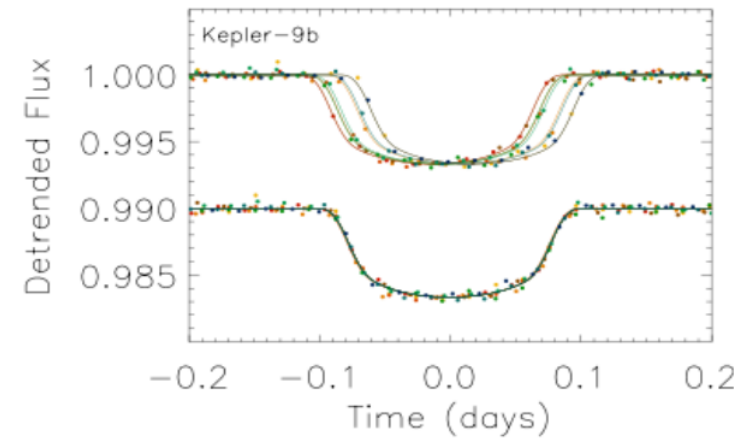
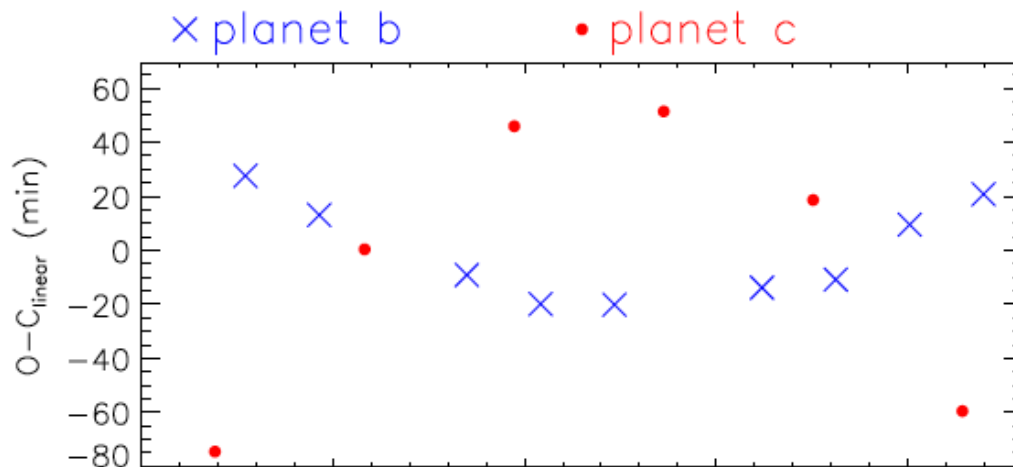


(Agol et al., 2005:
MNRAS, **359**, 567)

A. Ofir: TTV in Kepler data

Kepler-9:

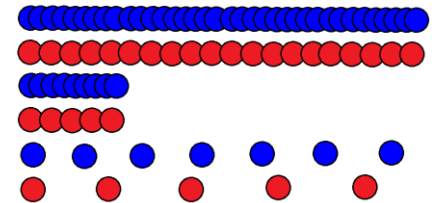
$P_b = 19.24$ d, $P_c = 38.91$ d (2:1 resonance)



A. Ofir: TTV in Kepler data

Kepler-9: better results with 6x more data (arXiv:1403.1372)

Kepler-9	Transits per planet		Total days	$M_c [M_{\text{Earth}}]$
	b	c		
Full data	68	36	1 400	31 ± 1
Partial data	9	6	200	55 ± 3
Diluted data	9	6	1 400	33 ± 2



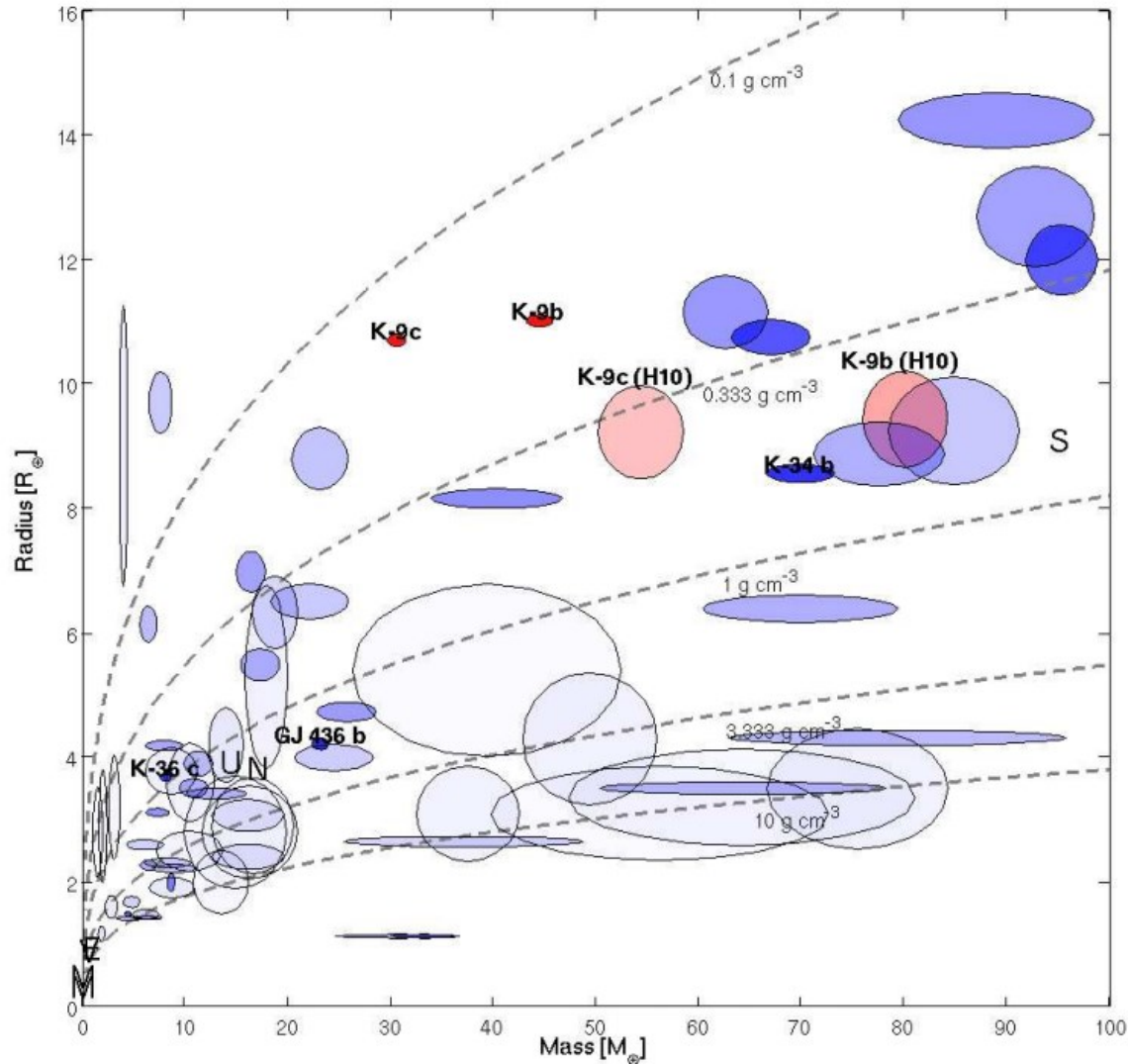
New R larger, new $M \sim 55\%$ smaller

Error limit of Kepler: $M_P \sim 2.8\%$, $R_P \sim 0.2\%$

Large TTVs even without MMR:

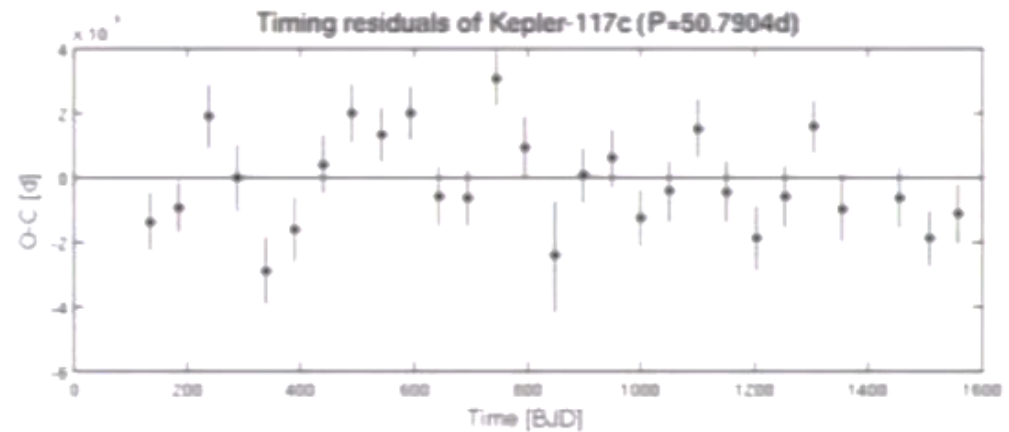
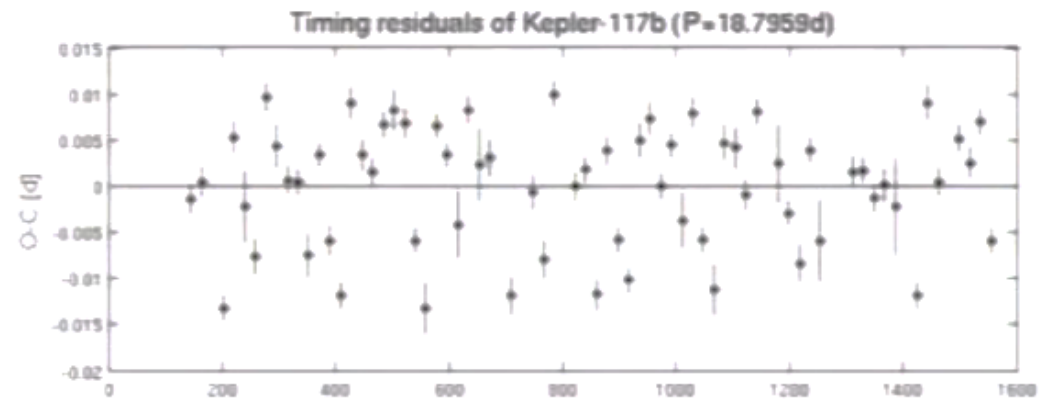
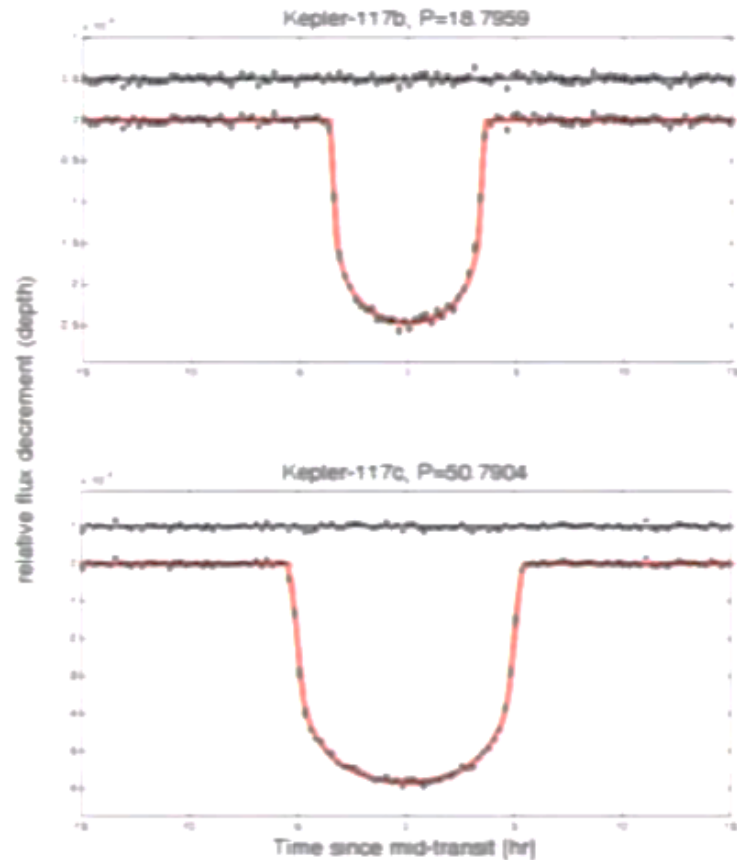
Catalog of Kepler TTVs (Mazeh, 2013: *ApJS*, **208**, 16)

A. Ofir: TTV in Kepler data



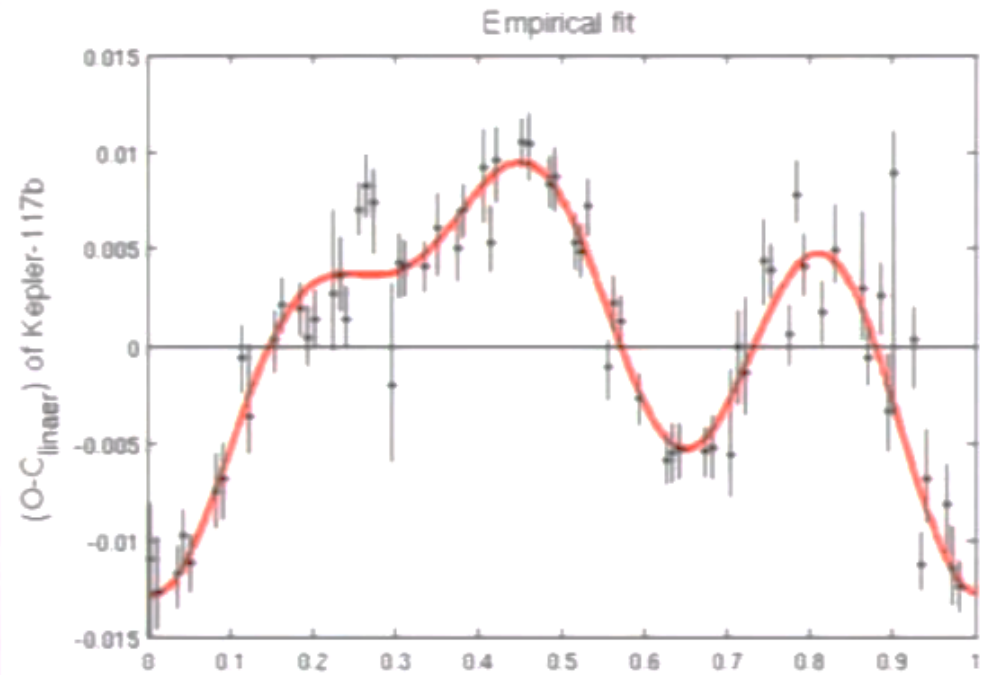
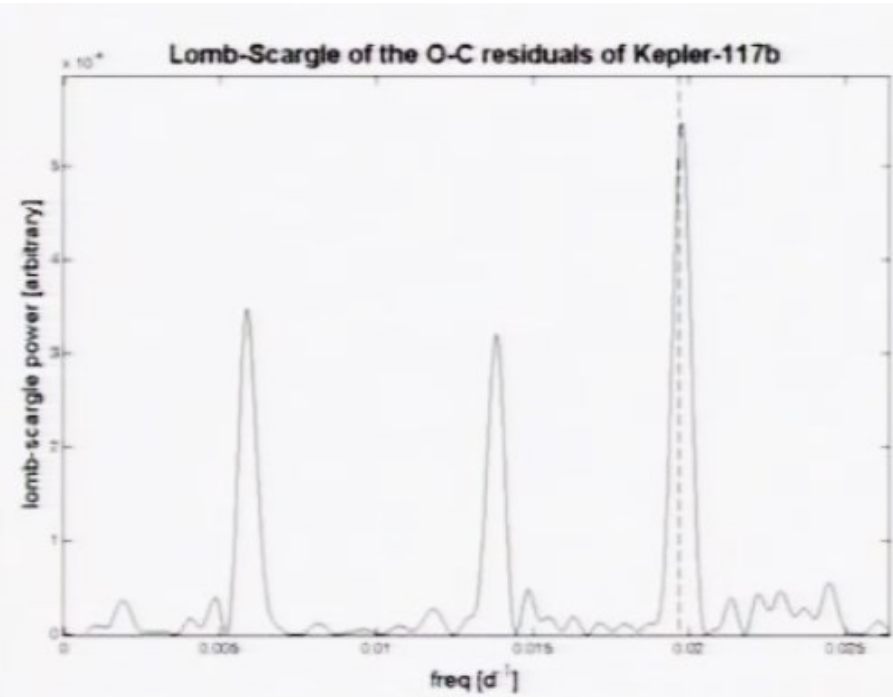
A. Ofir: TTV in Kepler data

Kepler-117



A. Ofir: TTV in Kepler data

Kepler-117



A. Ofir: KOINet



Primary for 1m+ class telescopes (13-15 mag)

Distinguish TTVs

<http://koinet.astro.physik.uni-goettingen.de/>

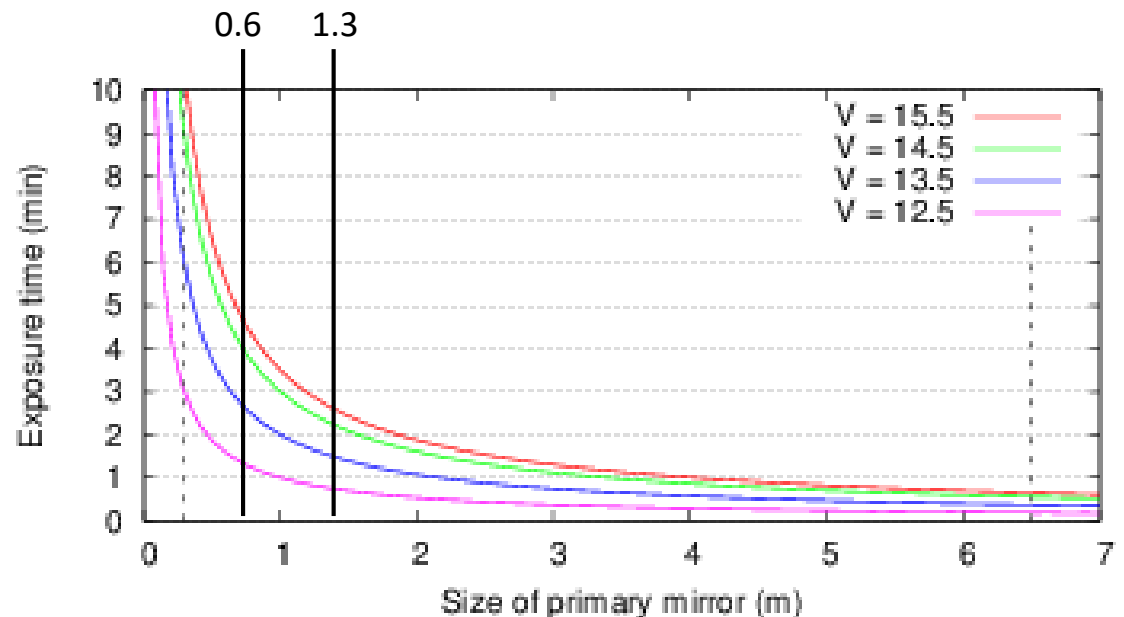
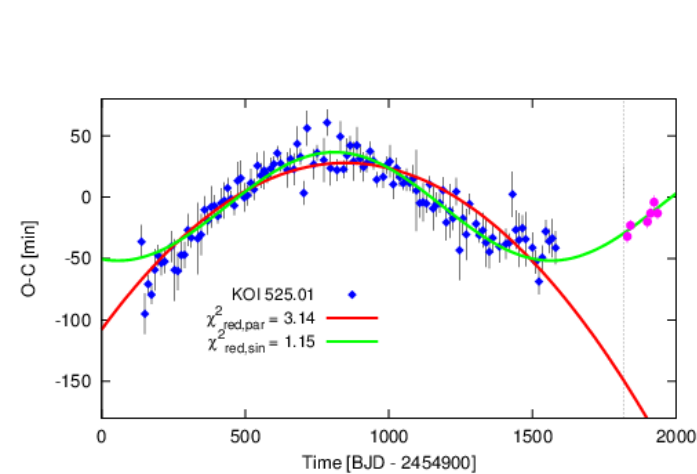


Figure 1: Estimation of exposure time as a function of primary mirror diameter for different values of apparent magnitude. Vertical lines indicate our network's largest and smallest telescopes.

J. Cabrera: CoRoT-29b

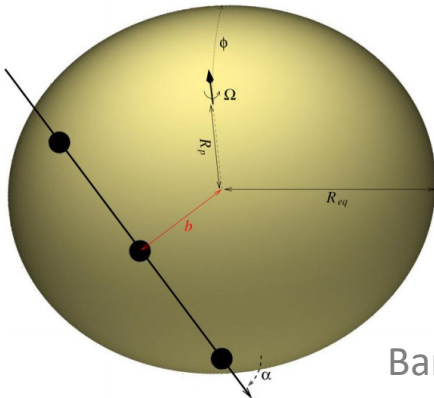
Peculiar transit (95% conf. level)

Asymmetry confirmed from ground

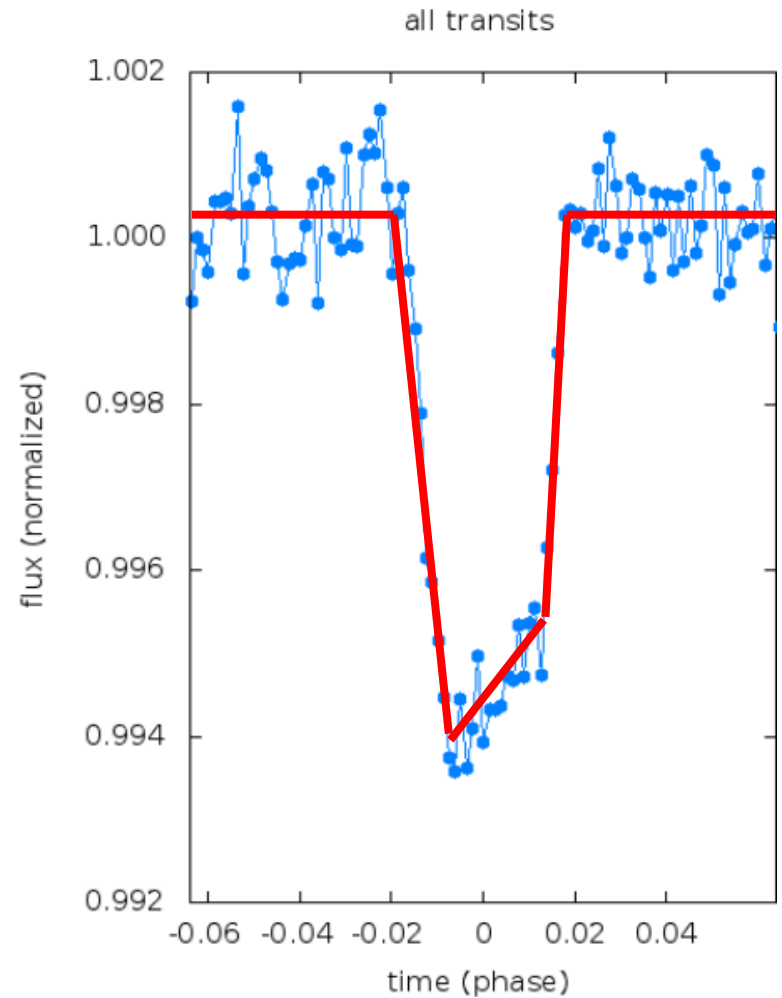
Ruled out:

- Tidal distortion of planet
- Stellar spots ($v \sin i \sim 3.5$ km/s)
- Evaporation

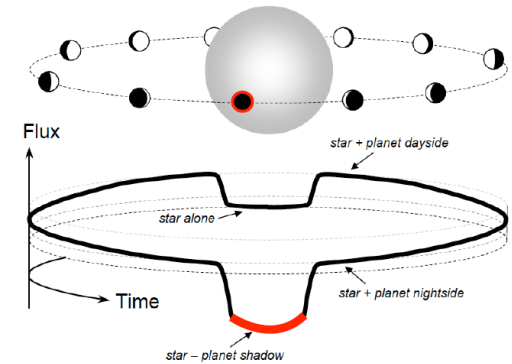
Maybe: gravity darkening?



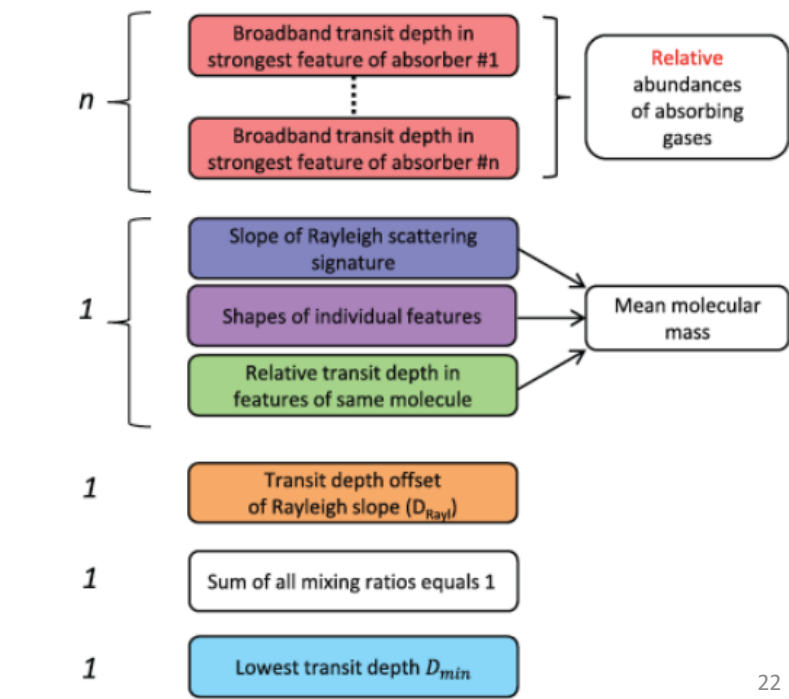
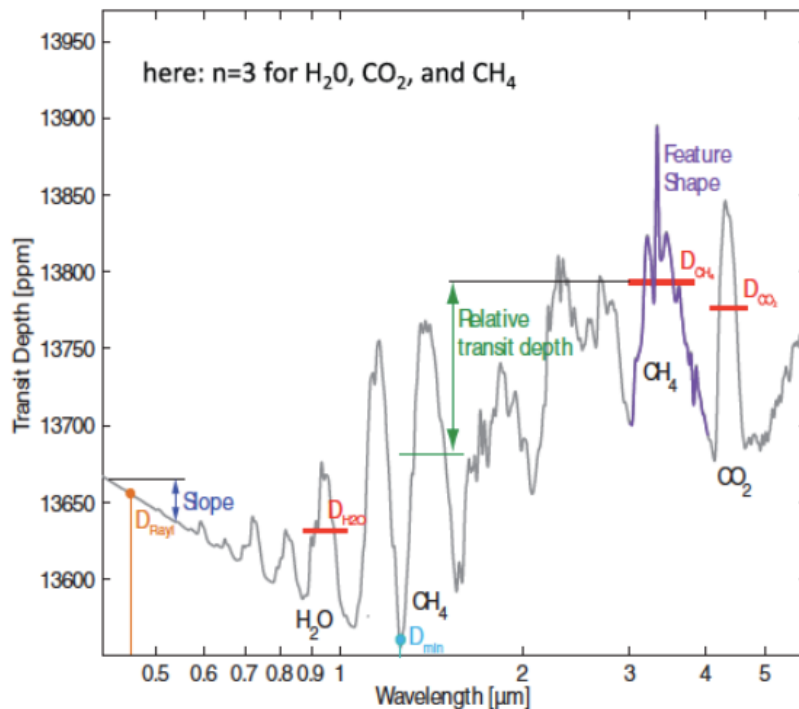
Barnes, 2009: *ApJ*, **705**, 683



K. Heng: Exoplanet atmospheres from optical data



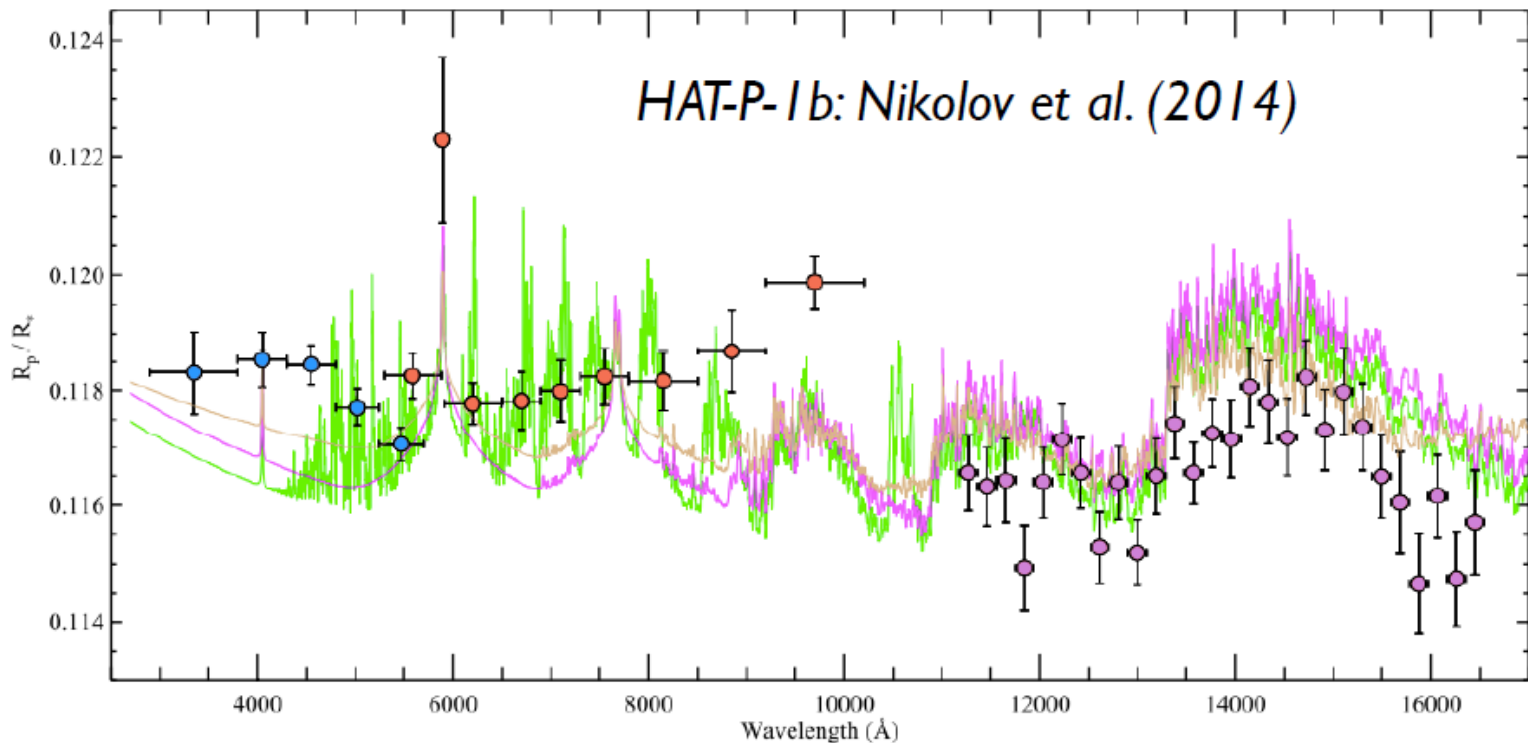
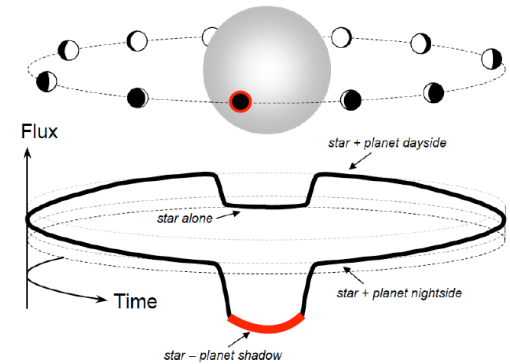
(Benneke & Seager, 2012: *ApJ*, 753, 100)



K. Heng: Exoplanet atmospheres from optical data

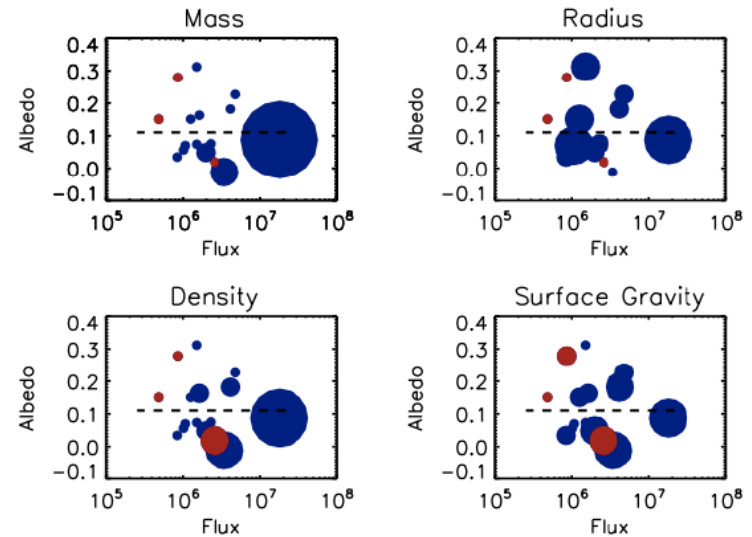
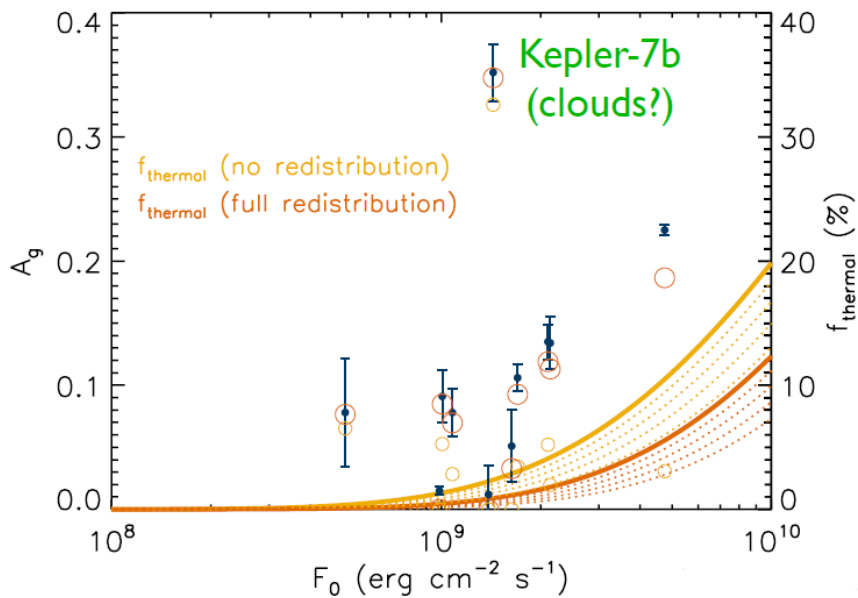
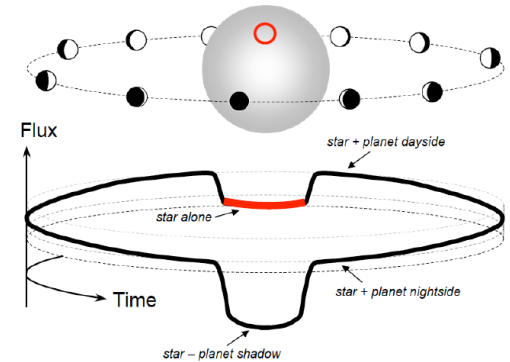
Some exoplanets are cloudy, some are not.
Unclear reasons.

(Nikolov et al., 2014: *MNRAS*, **437**, 46)



K. Heng: Exoplanet atmospheres from optical data

No trend of A with stellar irradiation, M , R , ρ , g
 Superearths appear more reflective than Jupiters.



(Heng & Demory, 2013: *ApJ*, **700**, 100)

(arXiv: 1404.4348)

M. Havel: CEPAM – planetary evolution model

Constrains properties of CoRoT stars and planets

New 1D EOS and atmospheric boundary conditions (M, R, L, T-P, g, rot)

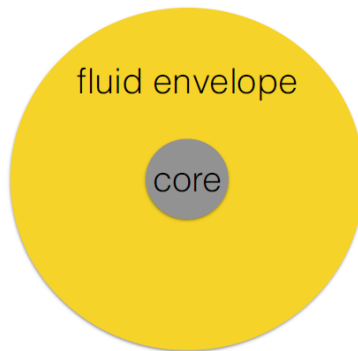
1-D equations:

$$\frac{\partial P}{\partial m} = -\frac{Gm}{4\pi r^4}$$

$$\frac{\partial T}{\partial m} = \left(\frac{\partial P}{\partial m}\right) \frac{T}{P} \nabla_T,$$

$$\frac{\partial r}{\partial m} = \frac{1}{4\pi r^2 \rho},$$

$$\frac{\partial L}{\partial m} = \dot{\epsilon} - T \frac{\partial S}{\partial t},$$

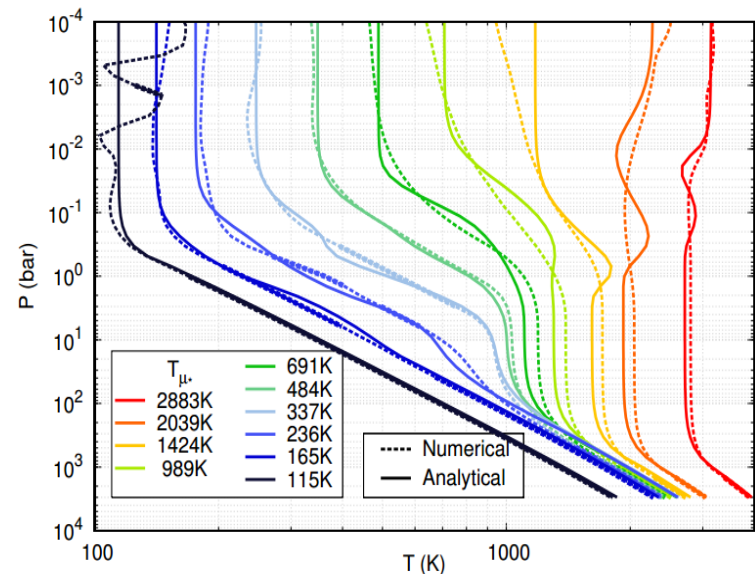


$$\rho = \rho(P, T, \{X_i\}); \quad S = S(P, T, \{X_i\})$$

$$m = 0 \rightarrow r = L = 0$$

$$m = M \rightarrow P = P_{\text{phot}}(g, L)$$

$$T = T_{\text{phot}}(g, L)$$



$T \in \langle 200, 2200 \rangle$ K, $M \in \langle 0.1, 10 \rangle M_J$, $Z \in \langle 0, 0.5 \rangle$, $L_{\text{dissip}} \in \langle 0, 0.5 \rangle$, $t \in \langle 0, 14 \rangle$ Gyr

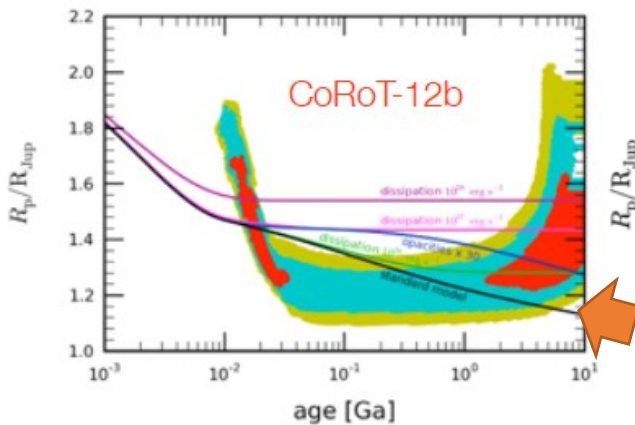
WARNING: Various exoplanet catalogs have different data for the same objects.

M. Havel: CEPAM – planetary evolution model

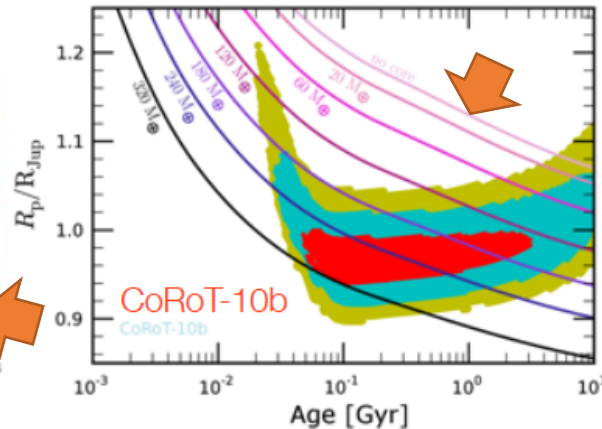
Categories of giant exoplanets:

- Inflated (155 of 249) $R_{\text{anom}} = R_{\text{obs}} - R_{\text{pred}} \sim T_{\text{eq}}^{1.4 \pm 0.6}$ (Laughlin, 2011: *ApJ*, 729L, 7)
- Massive core
- Young

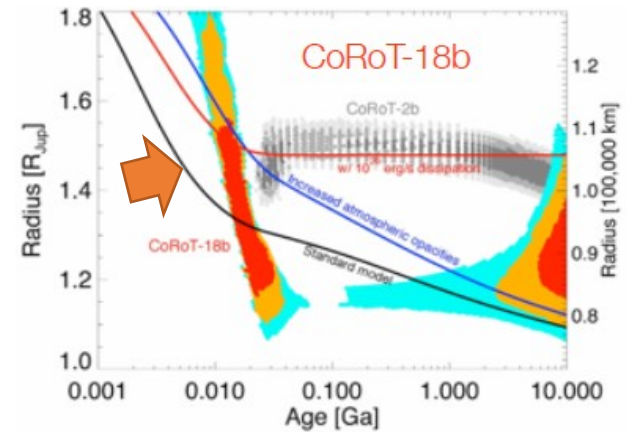
Inflated



Massive Core



Young

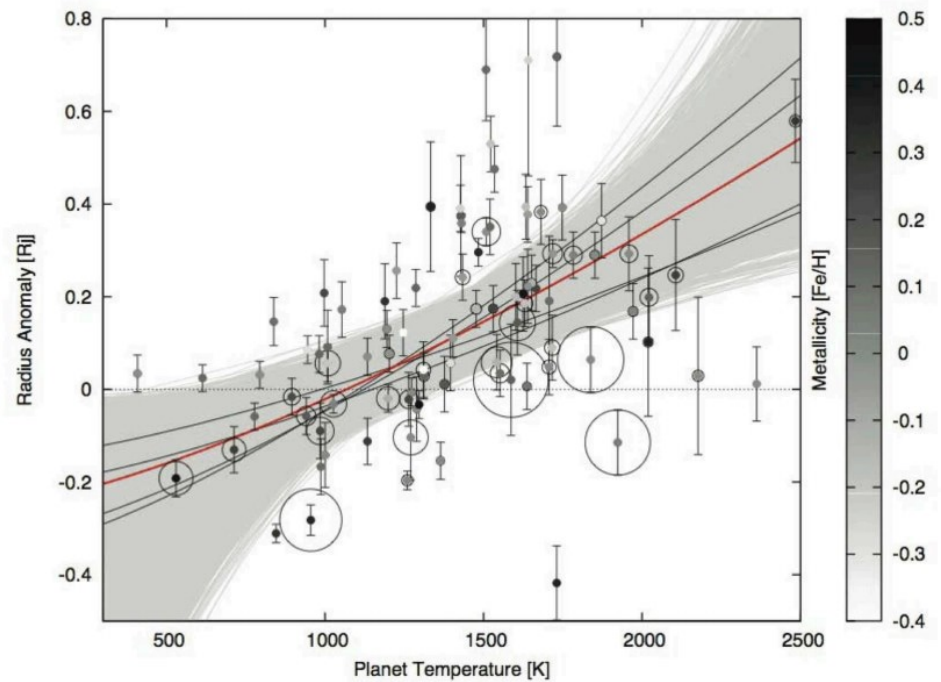
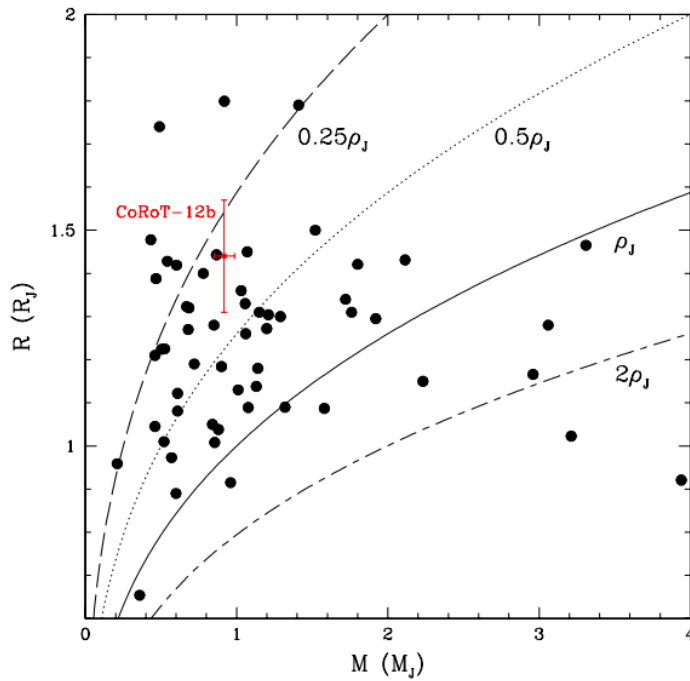


(Gillon et al., 2010: *A&A*, 520, 97) (Bonomo et al., 2010: *ApJ*, 520, 65) (Hébrard et al., 2011: *ApJ*, 533, 130)

M. Havel: CEPAM – planetary evolution model

Inflation mechanisms:

- Stellar-flux dissipation
- Tidal dissipation
- Delayed contraction



V. Parmentier: Cloudy atmospheres

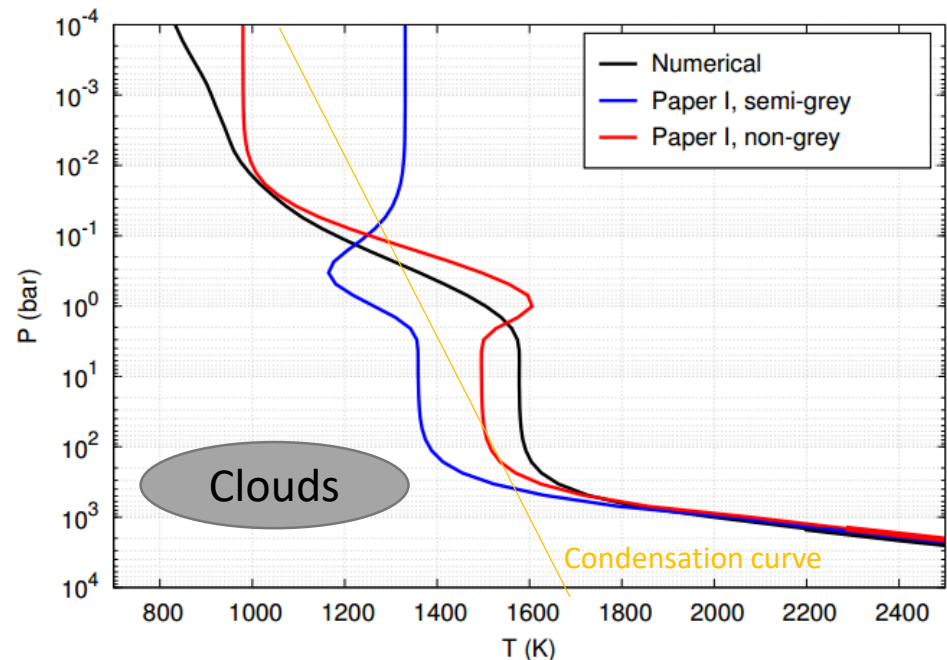
Presence of clouds in exoplanet's atmospheres is ubiquitous

Known planets: HD209458b (Deming, 2013: *ApJ*, **774**, 95), Kepler-7b (Demory, 2013: *ApJ*, **776**, 25), HD189733b (Sing, 2009: *A&A*, **505**, 891)

Techniques: transmission spectroscopy, albedo (and combination)

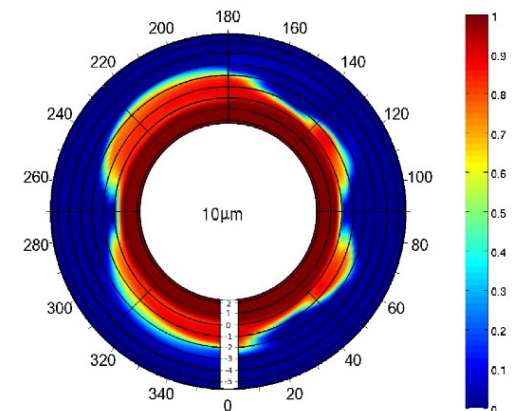
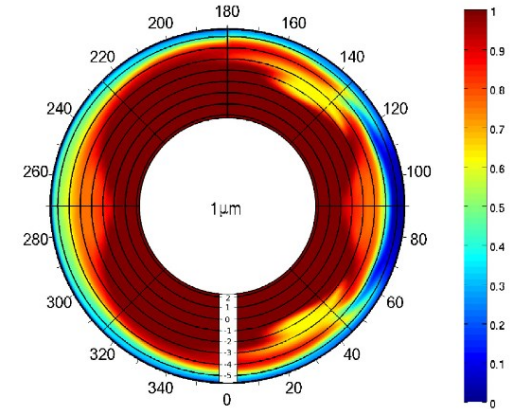
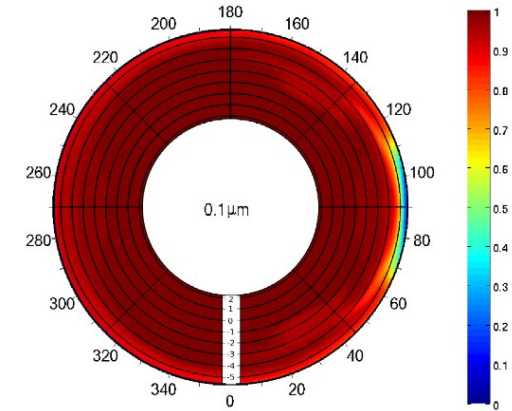
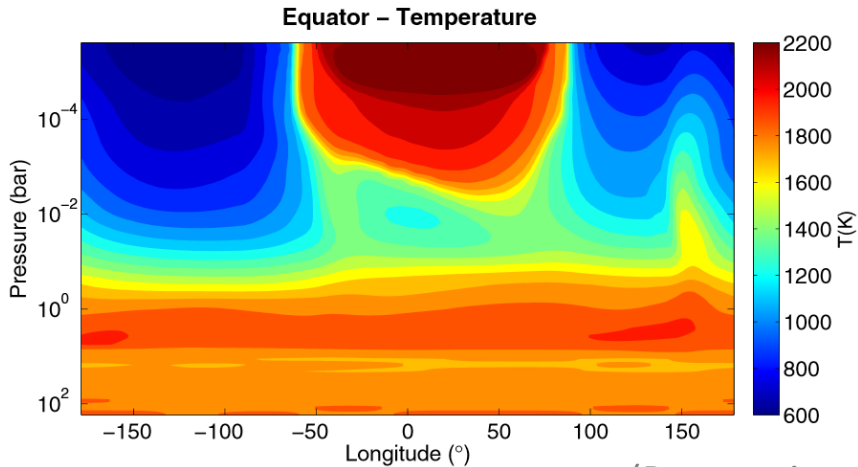
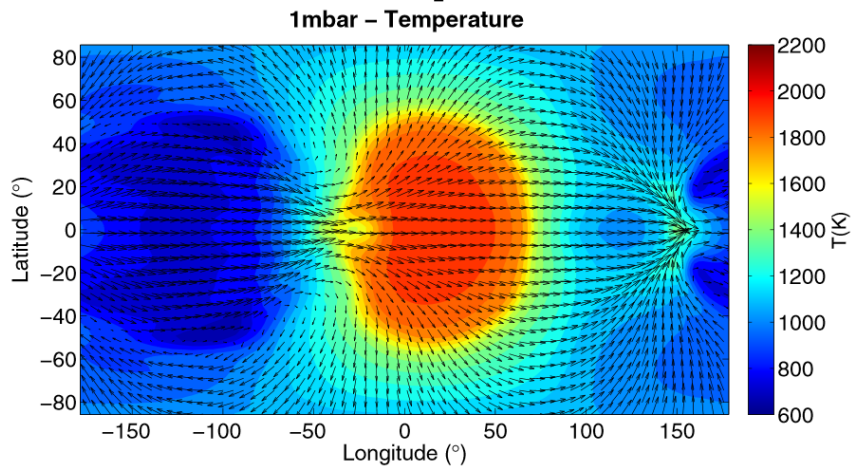
Clouds:

- If PT crosses condensation
- At limb?
- Partly on day-side
 - Longitudinal variations
 - Latitudinal variations



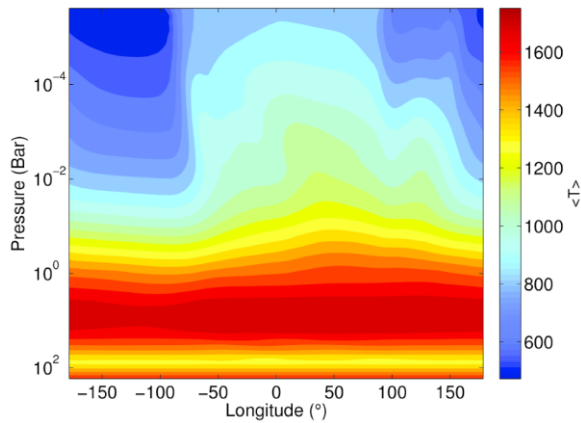
V. Parmentier: Cloudy atmospheres

HD209458b ($T_{\text{eq}} \sim 1500$ K) – limb clouds?

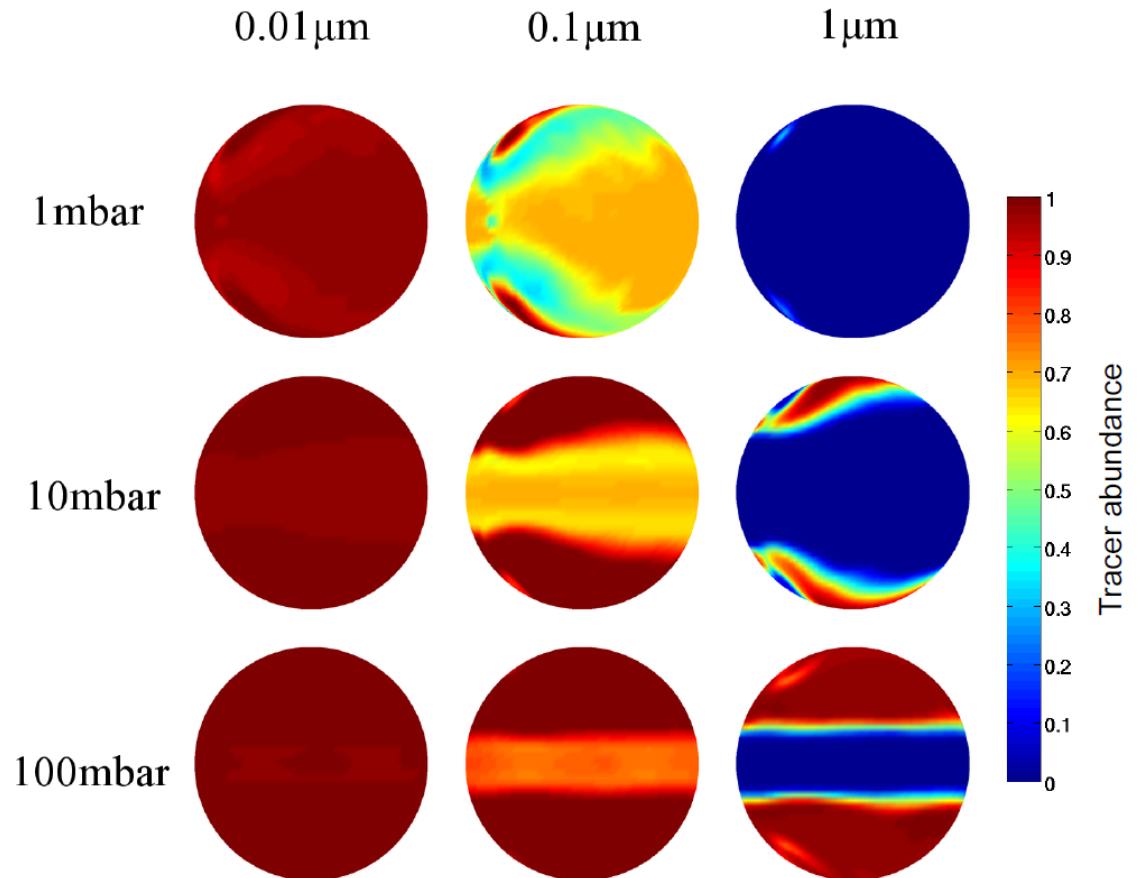


V. Parmentier: Cloudy atmospheres

HD189733b ($T_{\text{eq}} \sim 1200$ K) – latitudinal variations



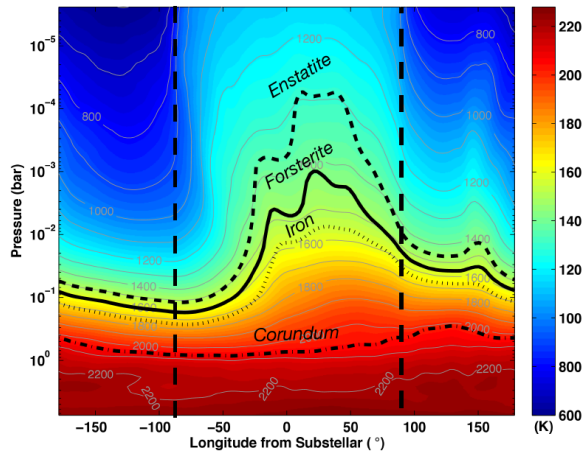
(Parmentier et al., in prep.)



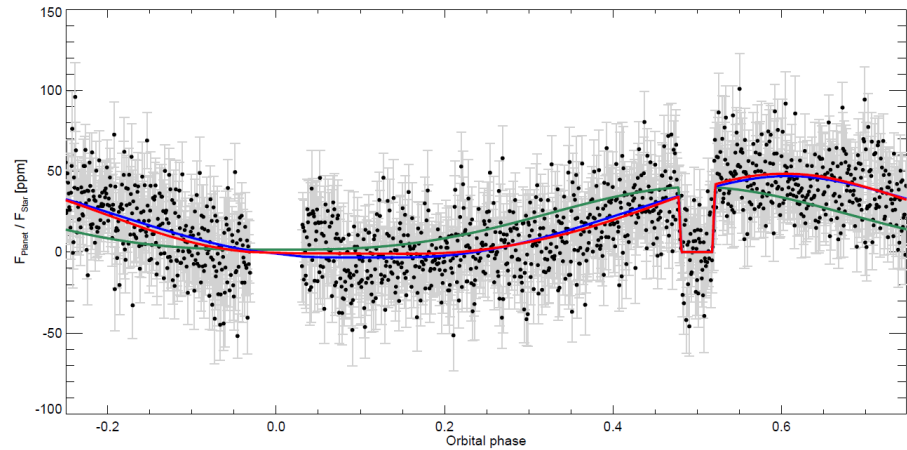
V. Parmentier: Cloudy atmospheres

Kepler-7b ($T_{\text{eq}} \sim 1300$ K, $A_g \sim 0.35$) – longitudinal variations

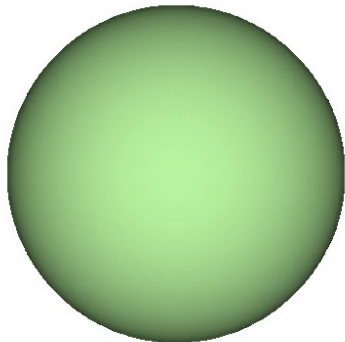
(Parmentier et al., in prep.)



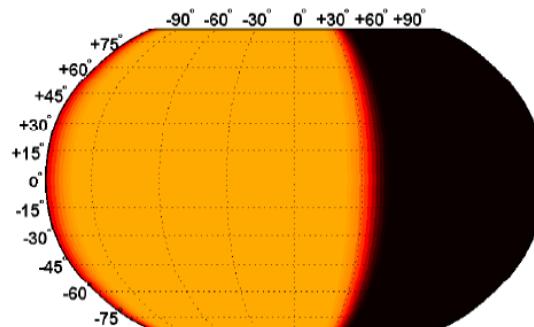
(Demory et al., 2013: *ApJ*, **776**, L25)



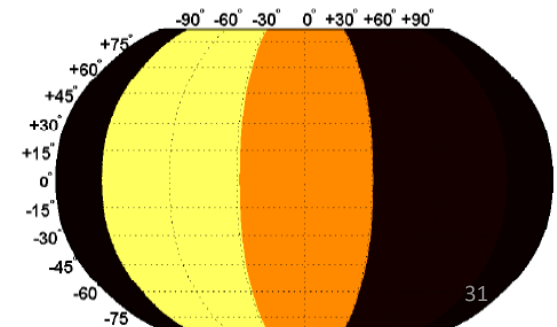
Lambertian sphere



Single band



Two bands



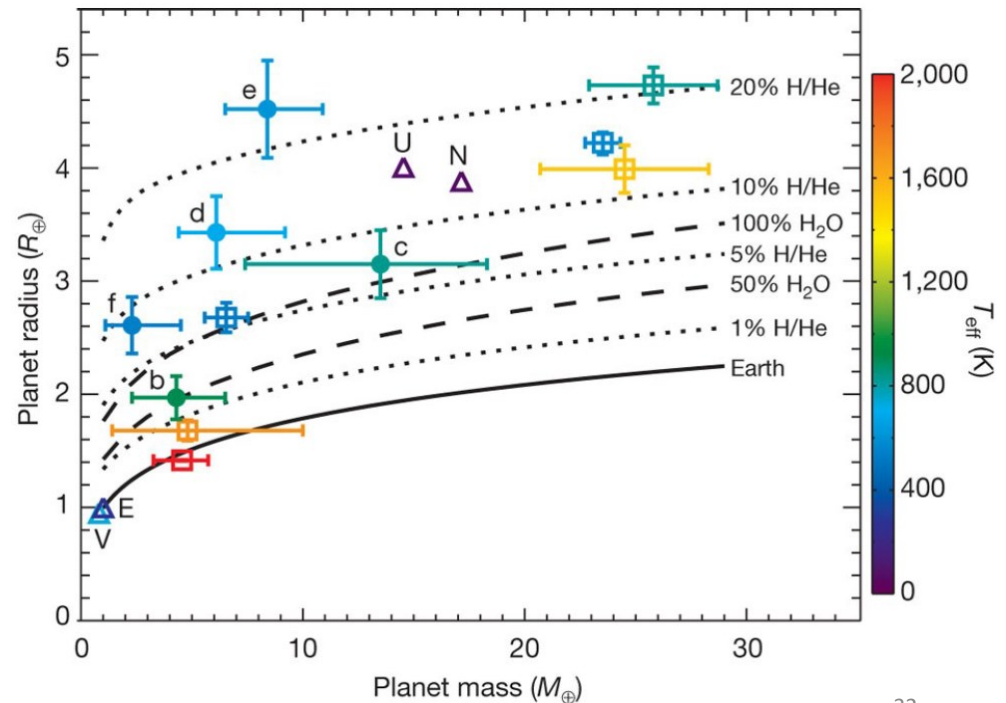
Sz. Csizmadia: Characterizing Exoplanets

Distinguish rocky/giant planets: 10% M , 5% R

Bulk characterization, interior structure of rocky planets: 2% R

Ubiquity in atmospheric studies: 0.1% R

$$\frac{\Delta F}{F} \cong \left(\frac{R_P}{R_{\star}} \right)^2$$



Sz. Csizmadia: Characterizing Exoplanets

Distinguish rocky/giant planets: 10% M , 5% R

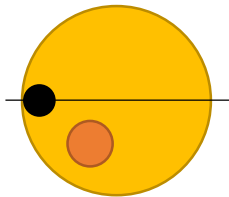
Bulk characterization, interior structure of rocky planets: 2% R

Ubiquity in atmospheric studies: 0.1% R

Gaia prediction: 2% R_{\star} (today host stars: 10 – 15% R_{\star})

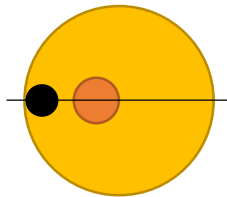
$$\frac{\Delta F}{F + F_{\text{contamination}}} = \left(\frac{R_P}{R_{\star}} \right)^2 \times L_D(u_a, u_b, x, y)$$

Type I



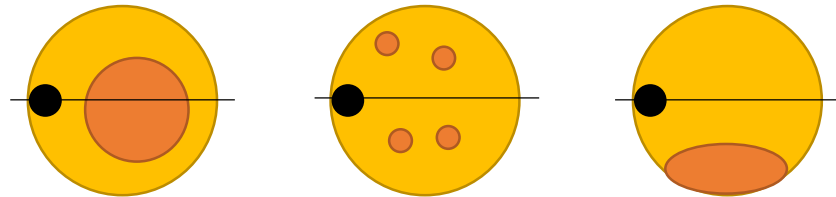
(Czesla et al.,
2009: *A&A*, **505**, 1277)

Type II



(Silva-Valio & Lanza,
2010: *A&A*, **510**, 25)

Type III



(Jackson & Jeffries, 2012:
MNRAS, **423**, 2966)

Sz. Csizmadia: Characterizing Exoplanets

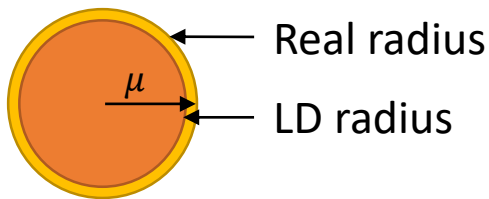
Distinguish rocky/giant planets: 10% M , 5% R

Bulk characterization, interior structure of rocky planets: 2% R

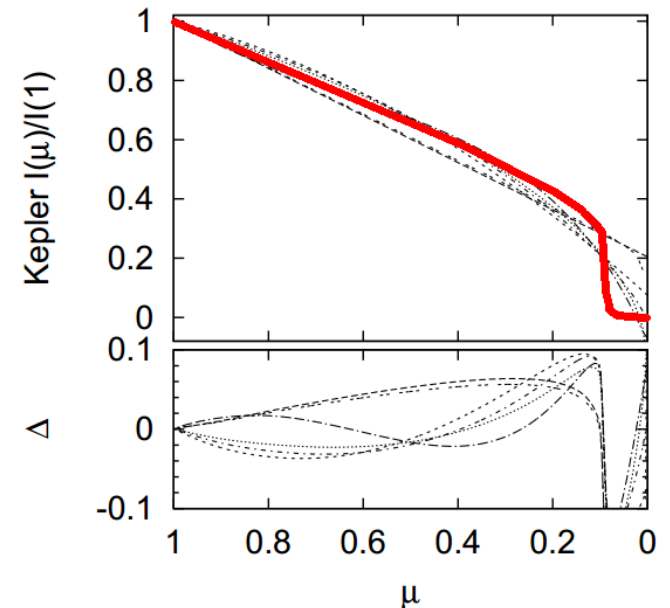
Ubiquity in atmospheric studies: 0.1% R

$$\frac{\Delta F}{F + F_{\text{contamination}}} = \left(\frac{R_P}{R_{\star}}\right)^2 \times L_D(u_a, u_b, x, y)$$

Giants and dwarfs:



Giants can even have limb brightening!

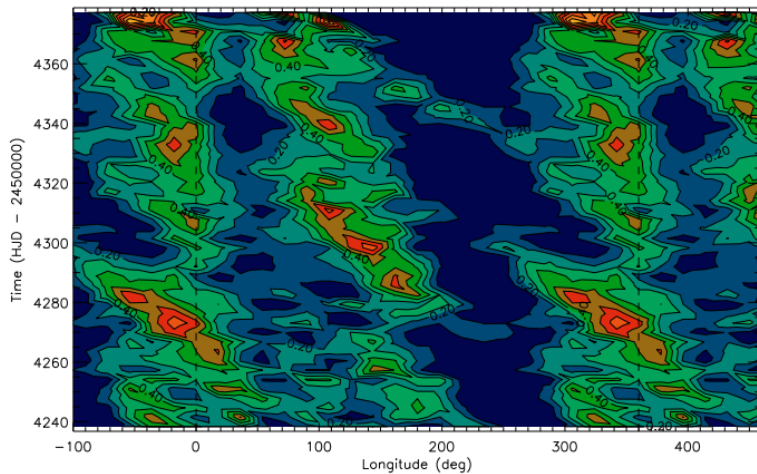


Neilson & Lester (arXiv:1305.1311)

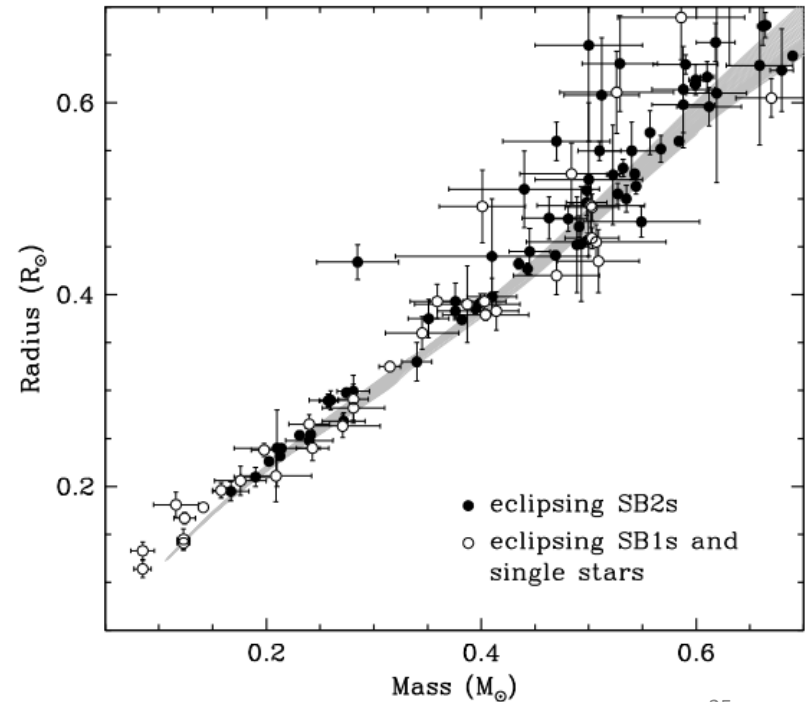
Sz. Csizmadia: Characterizing Exoplanets

Spots change: T_{eff} , R_{\star} , M-R relation (Torres, 2013: *AN*, **334**, 4)

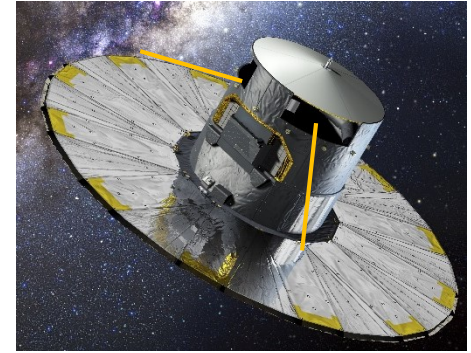
Spot-fitting map of CoRoT-2 (Lanza, 2009: *A&A*, **493**, 193)



Parameter	Typical error
T_{eff}	100 K
$\log g$	0,1
$[M/H]$	0,1
LD	5%



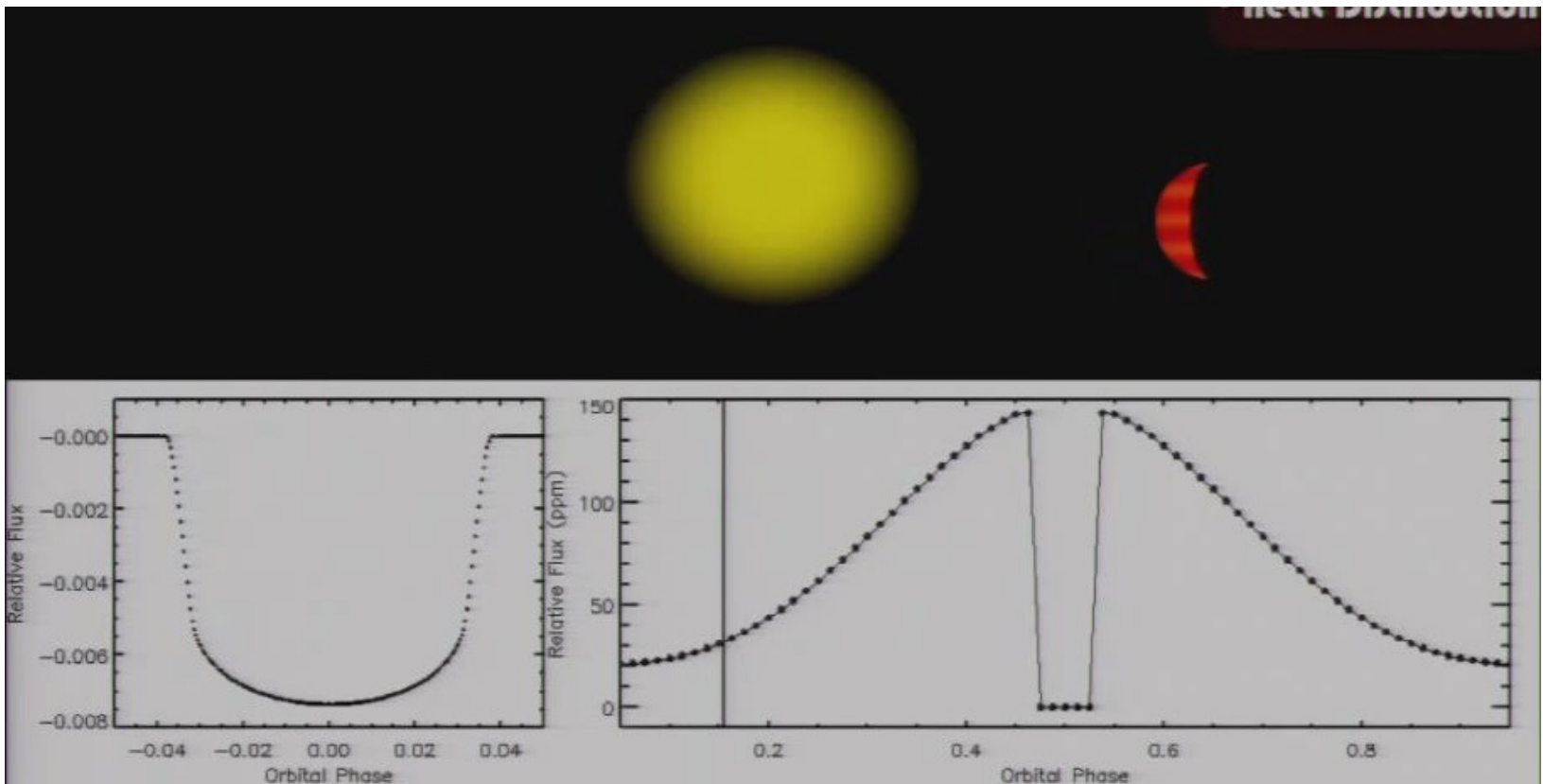
A. Sozzetti: Gaia



- Launched: 19.XII.2013
- FOV: 0,75 deg² (4 500 x 1 960 pix)
- Precision 20 μ arcs up to 12 mag
- First data delivery: V.2016
- Detection: $\sim 10^3$ exoplanets with short P_{orb} @ FGKM, capable of:
 - 2-3 M_J within 2-4 AU off star (<200 pc)
 - Saturn mas ($1/3 M_J$) within 1-4 AU off star (<25 pc) (Sozzetti, arXiv:1406.1388)
 - 10^9 stars up to 20 mag with 430 μ as astrometric precision
- Statistical reanalysis of planet occurrence found by *KEPLER* (Howard 2012: *ApJS*, 201, 15) as function of M_{\star} , $[M/H]$, $T_{\star,\text{eff}}$...
- Gaia DPAC Pipeline
- First major release (middle of 2016)

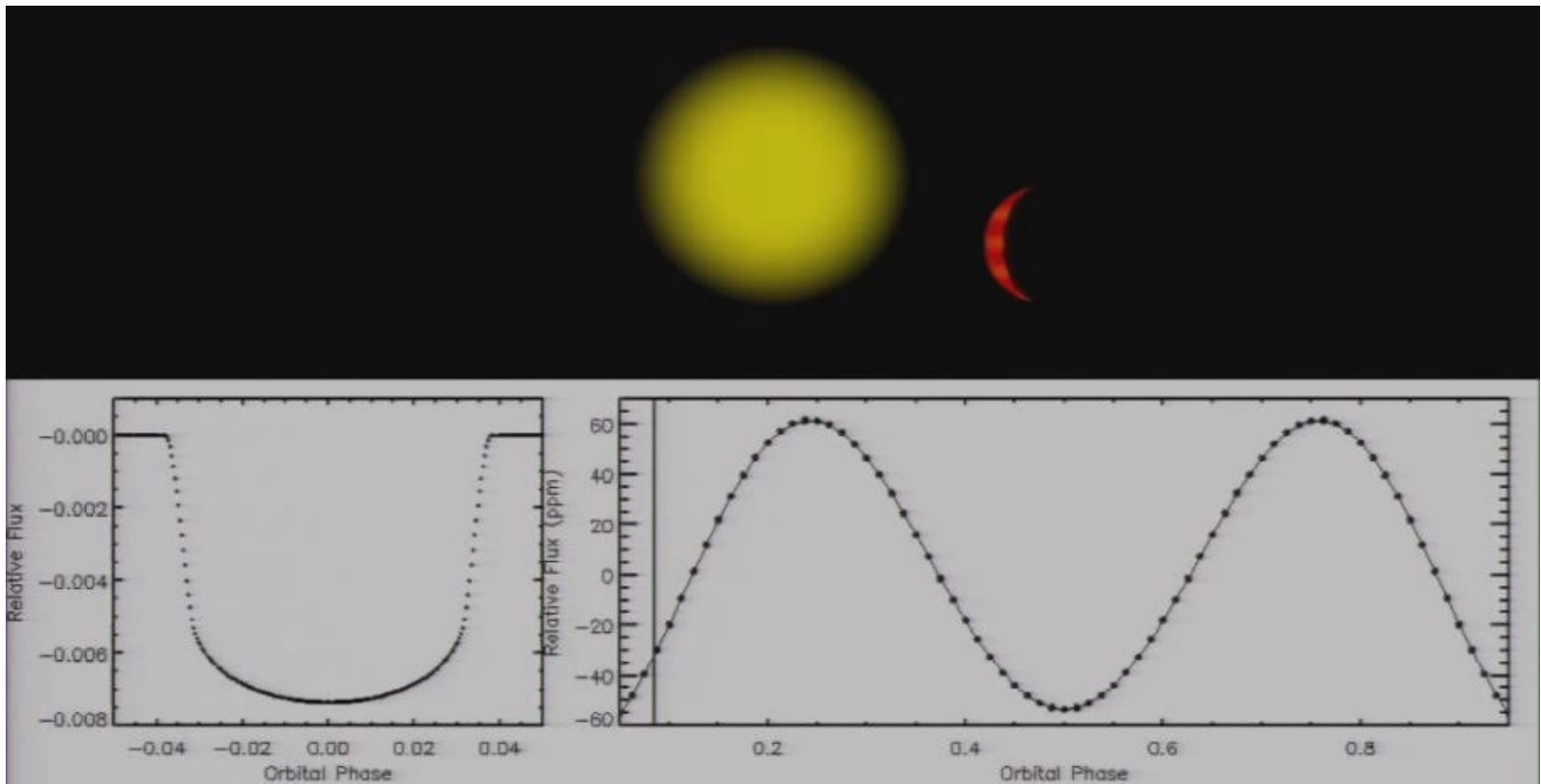
R. Jayawardhana: Planetary phase curves

Reflection + Thermal emission



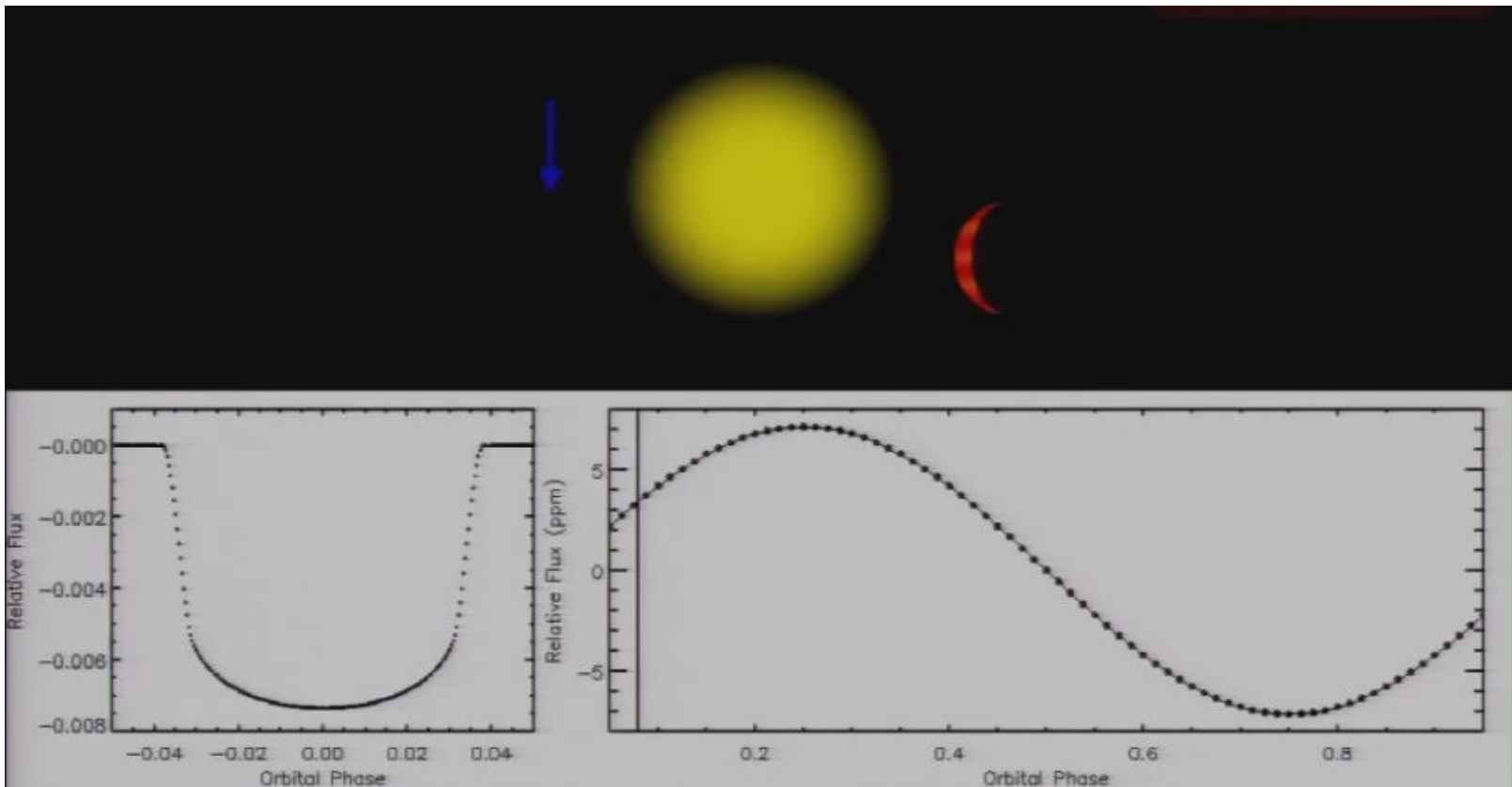
R. Jayawardhana: Planetary phase curves

Ellipsoidal variations



R. Jayawardhana: Planetary phase curves

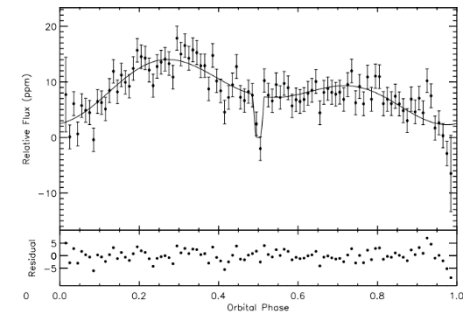
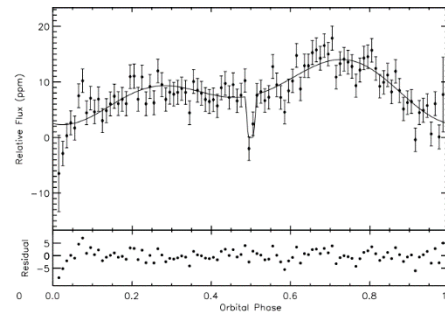
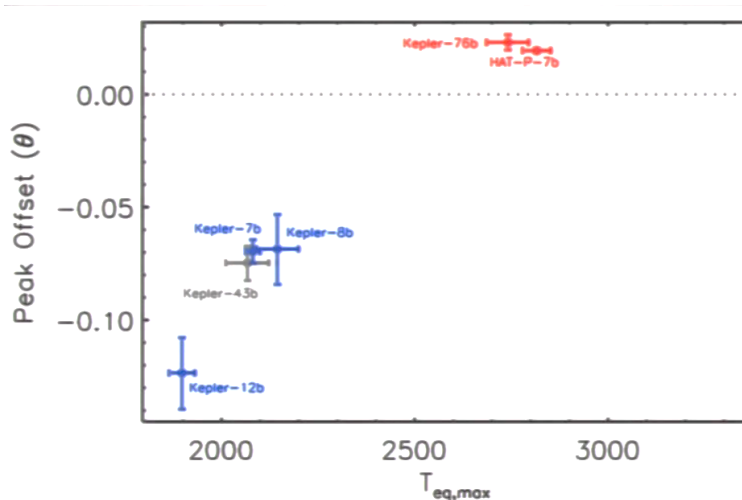
Doppler beaming



R. Jayawardhana: Planetary phase curves

Kepler + Spitzer – day/night variations: reflected light + thermal emission, ellipsoidal variations, Doppler beaming, e.g. Kepler-7b (Demory, 2013: *ApJ*, **776L**, 25) (others: 5,6,8,10,12,41,43,76,91,412)

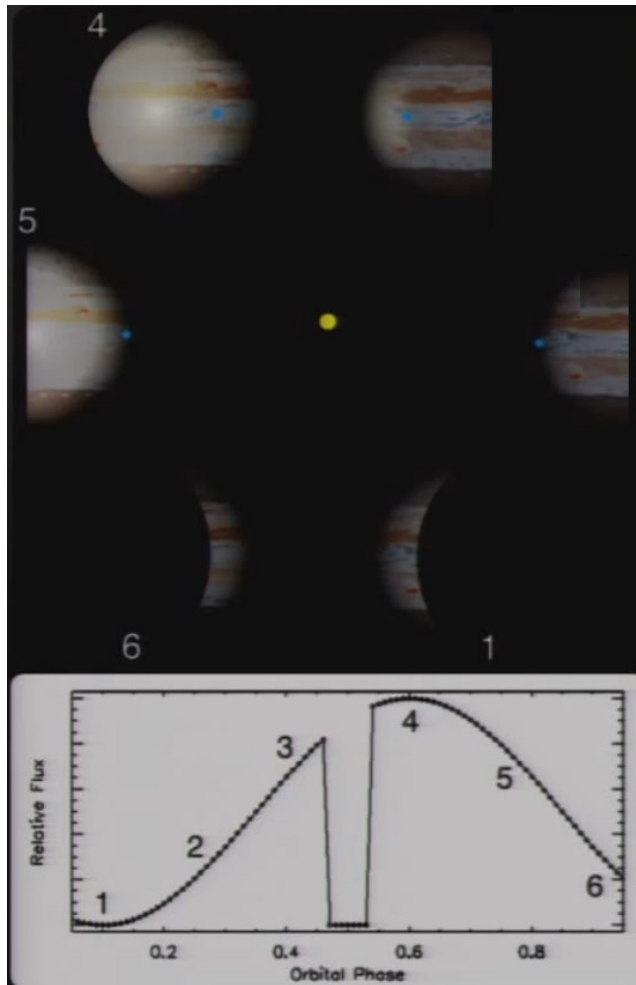
~50% of sample show offset of peak planetary light from the mid-eclipse (Esteves, 2013: *ApJ*, **772**, 51)



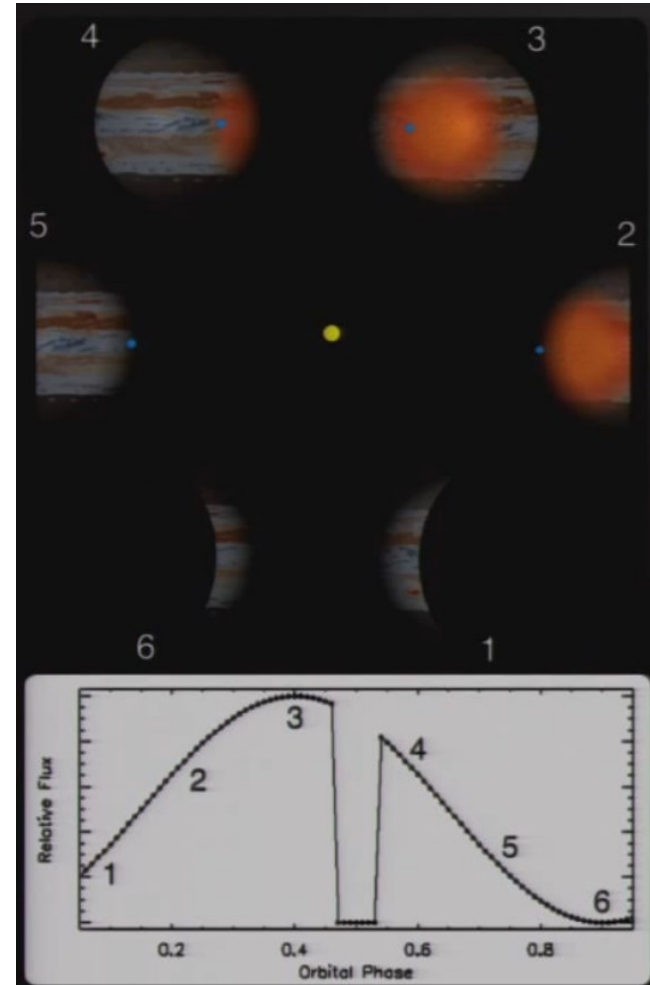
westward	clouds?	eastward
Winds contra-rotating		Winds co-rotating
$T_P < 2500$ K		$T_P > 2500$ K
Condense particles?		Cannot condense particles?
Dominant reflection		Dominant thermal emission

R. Jayawardhana: Planetary phase curves

westward



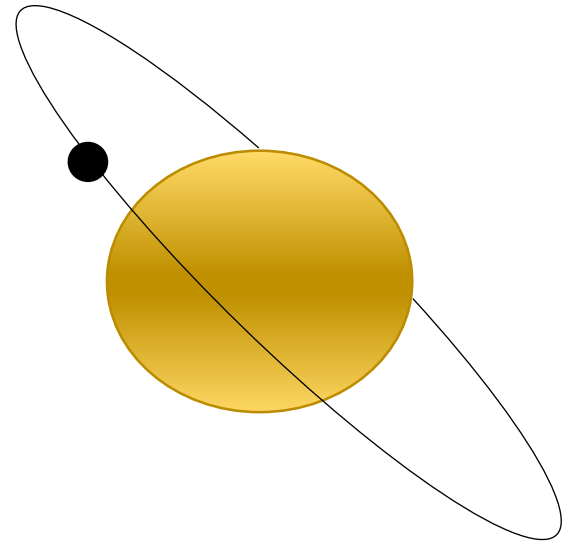
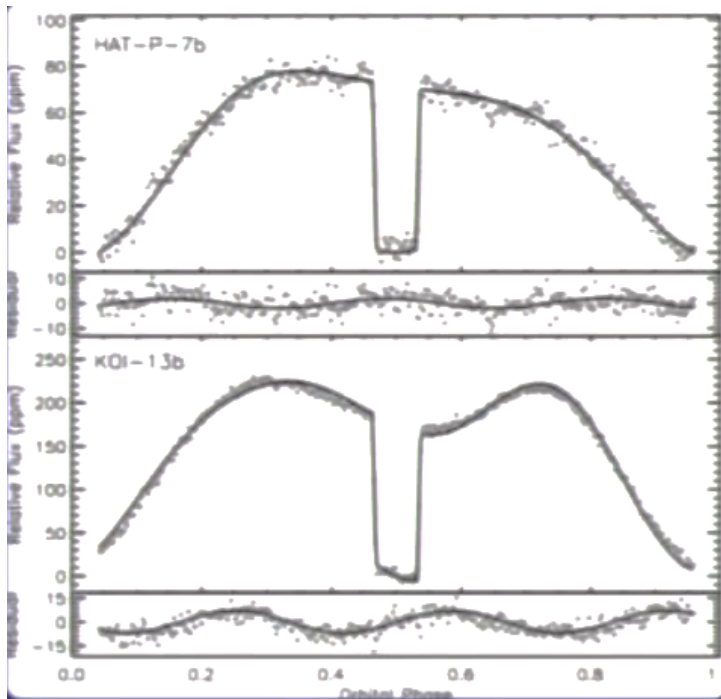
eastward



R. Jayawardhana: Planetary phase curves

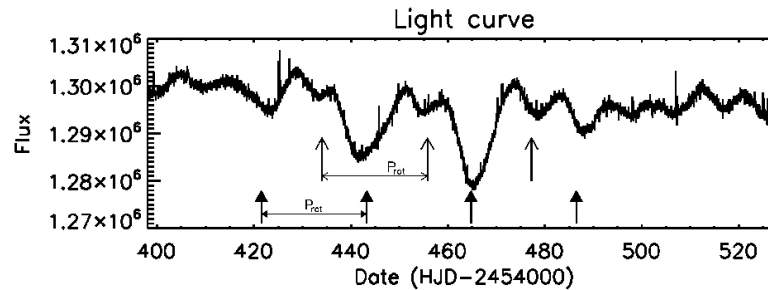
Case of KOI-13b and HAT-P-7b:

- Out-of-phase variation with $1/3 P_{\text{orb}}$
- Spin-orbital misalignment and gravity darkening (rotation)

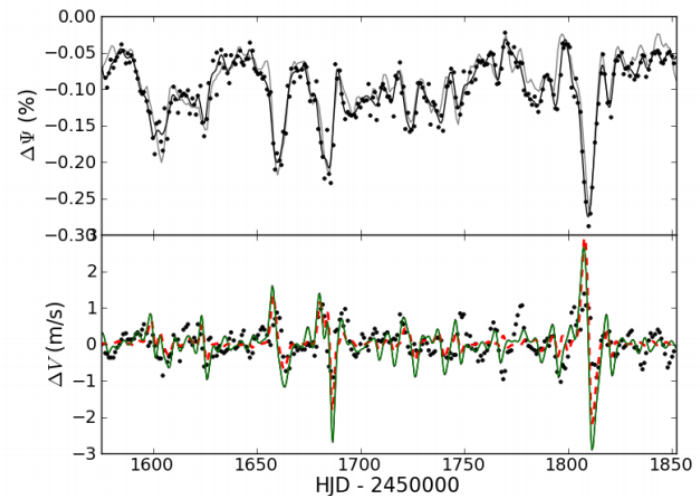
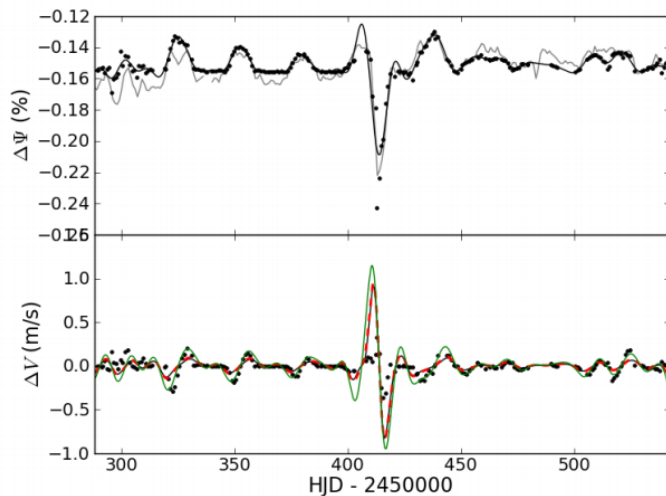


S. Barros: CoRoT-7b

First transiting super-Earth ($R_p = 1.585 \pm 0.064 R_E$)



Solar activity removed with FF' method (Aigrain et al., 2012: *MNRAS*, **419**, 3147)

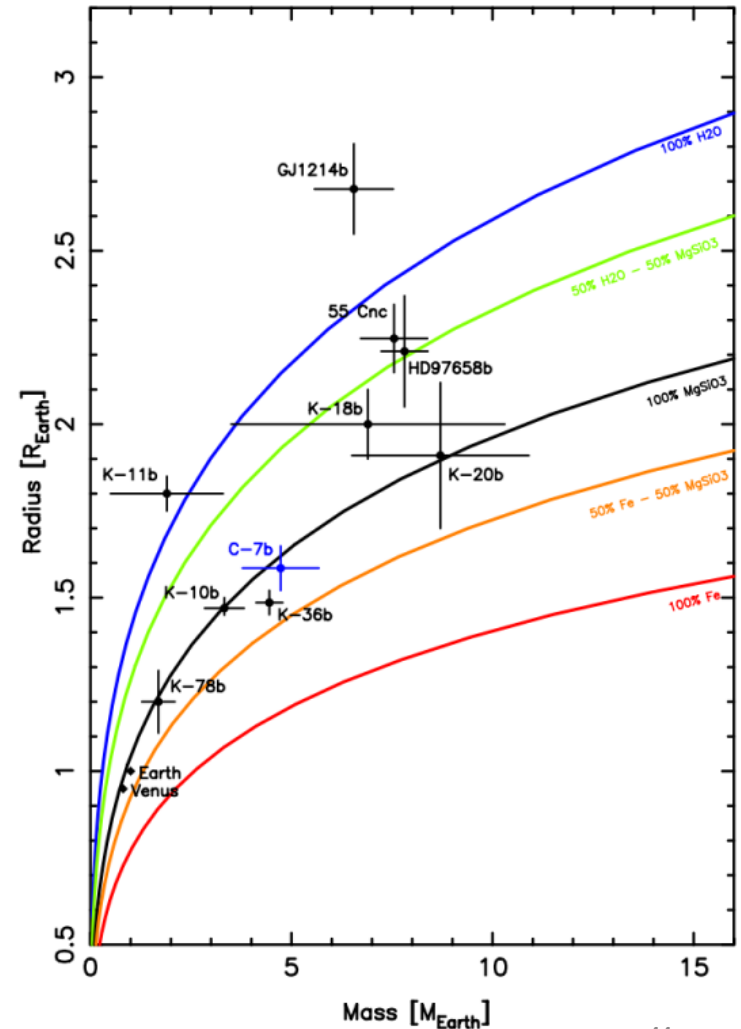
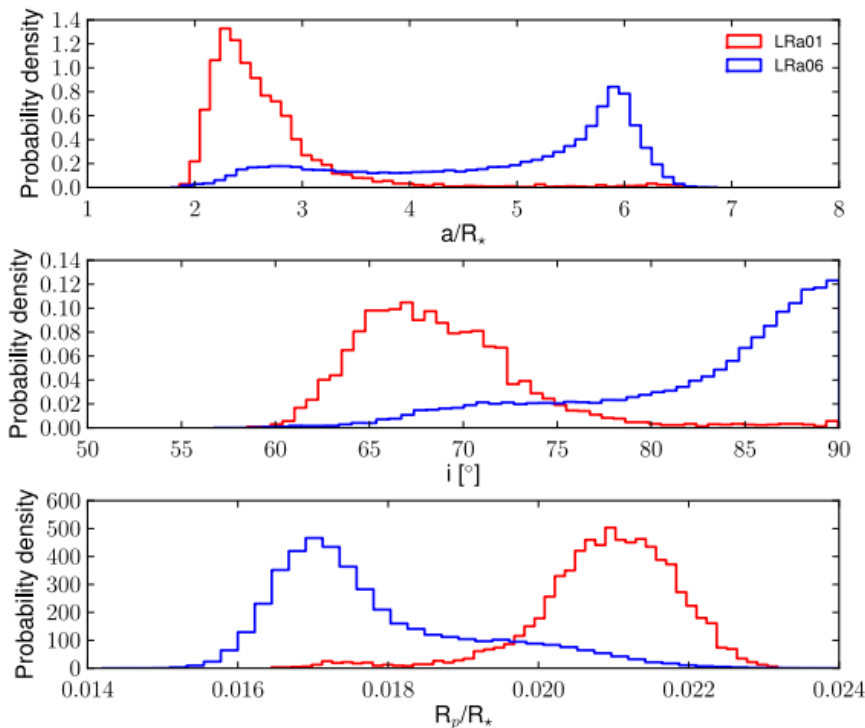


S. Barros: CoRoT-7b

Initial transits: $\rho_{\star} = 0.2 \rho_{\odot}$

New analysis: $\rho_{\star} = 1.6 \rho_{\odot}$

Ignoring stellar activity leads to an incorrect interpretation of the system



I. Baraffe:

Structure of exoplanets

M-R relation for terrestrial planets: $R \propto M^{0.274}$ (Sotin et al., 2007: *Icarus*, **191**, 337; Grasset et al., 2009: *ApJ*, **693**, 722)

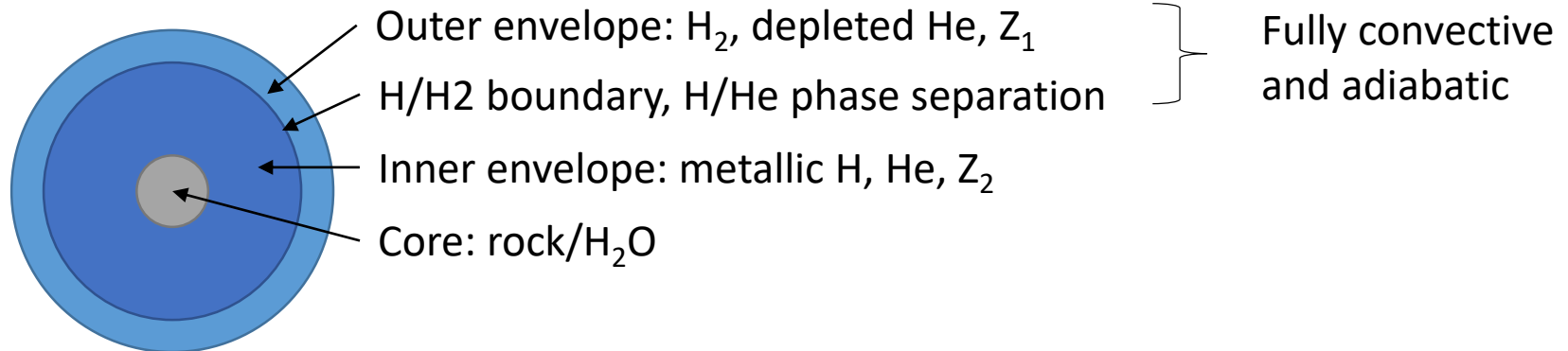
Used in exoplanet modelling:

- 1D atmospheric model (irradiated or not) – boundary conditions of the interior
- Atmospheric dynamics (Global Circulation Model) – ohmic dissipation, heating, mixing
- H/He envelope – EOS for H/He/Z, evolutionary models
- Rocky/ice core – EOS for H₂O, CH₄, NH₃, MgSiO₄, MgSiO₃, Fe ..., tectonics

Results for solar system:

- Jupiter: He depleted ($Y = 0.234$), Ar, Kr, Xe, C, N, S enriched (3-8 × solar)
- Saturn: He depleted ($Y = 0.18 - 0.25$), CH₄, NH₃ enriched (12-21 × solar)
- Agrees with the core accretion model

I. Baraffe: Structure of exoplanets



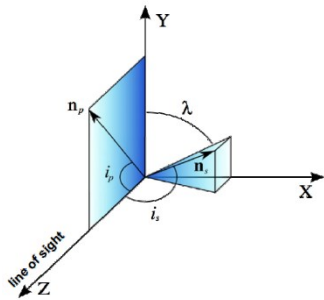
Molecular weight gradient (∇_μ) formed during accretion and stabilizes against convection, leads to much **fainter** planets!

Double diffuse (layered) convection – tiny diffuse layers prohibit heat dissipation (e.g. Saturn has higher L and 30%-60% higher Z than simple adiabatic model)

If Z equally distributed in core – 30% error in R! (Baraffe et al., 2008: *A&A*, **482**, 315)

C. Baruteau: Formation and evolution of planetary systems

Many misaligned hot Jupiters



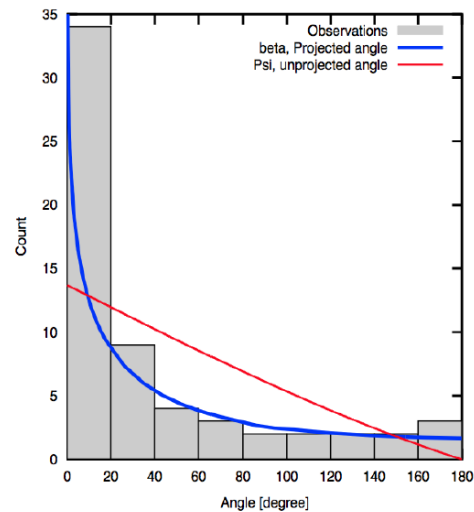
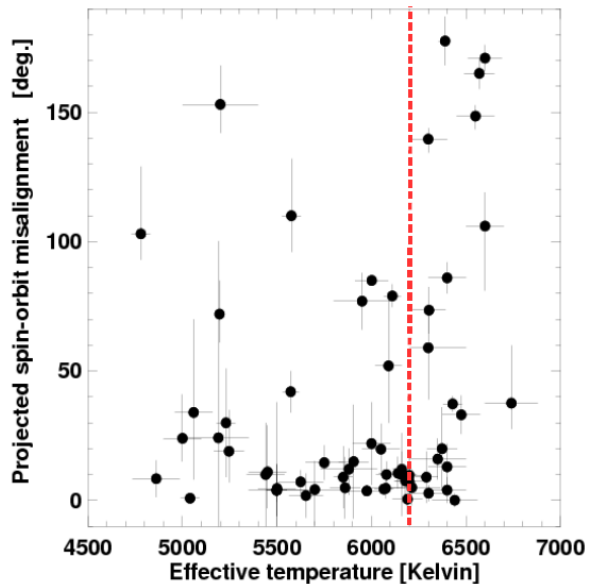
Disc migration – aligned

- Misaligned by nearby stars?

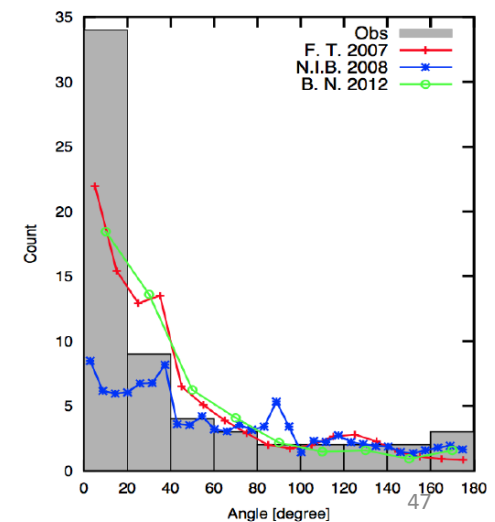
(Batygin, 2012: *Nature*, **491**, 418)

- Tidal flip of stellar spin axis?

(Barker & Lithwick, 2014: *MNRAS*, **437**, 305)



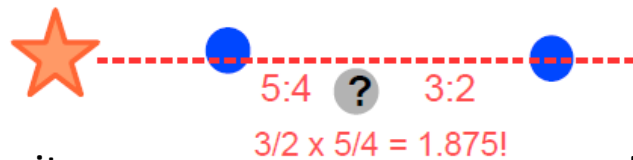
High-e migration – misaligned



C. Baruteau: Formation and evolution of planetary systems

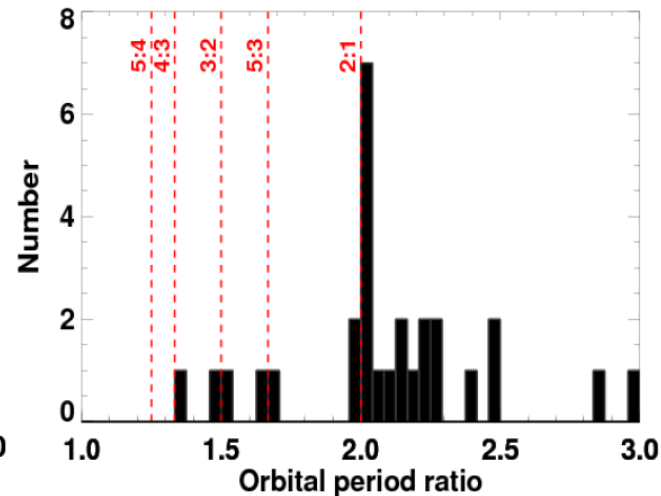
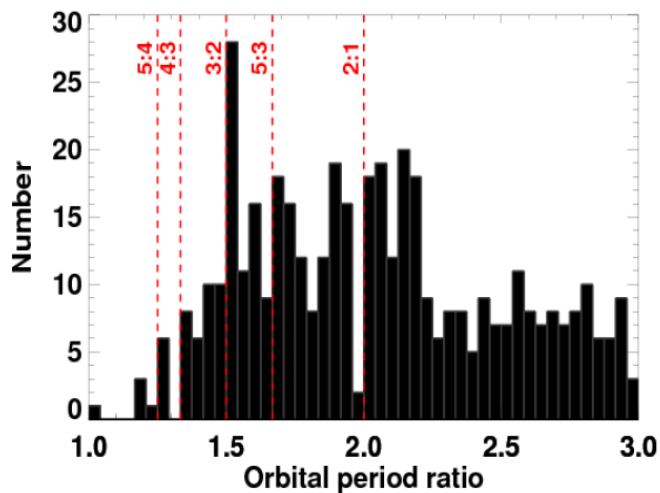
Orbital period resonances in multiple planetary systems

- Many not in resonance, but slightly wider of resonance
- Unseen companions? (Steffen, 2013: *MNRAS*, **433**, 3246)



Transits

RVs



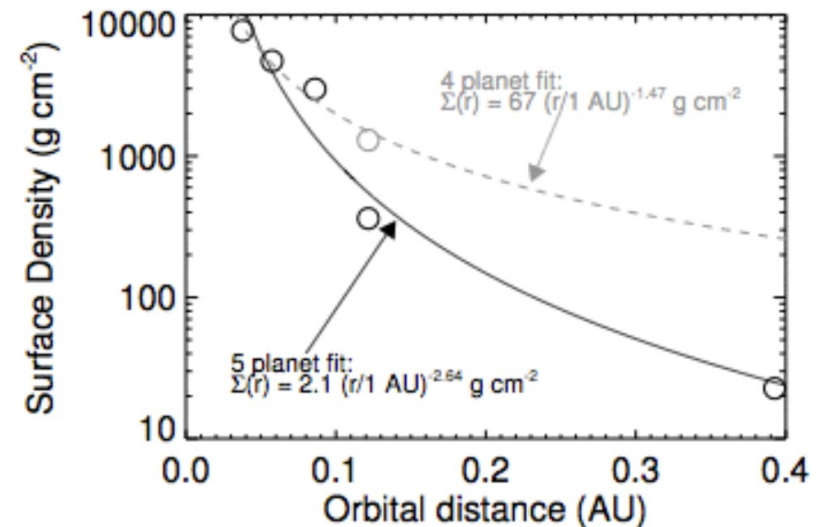
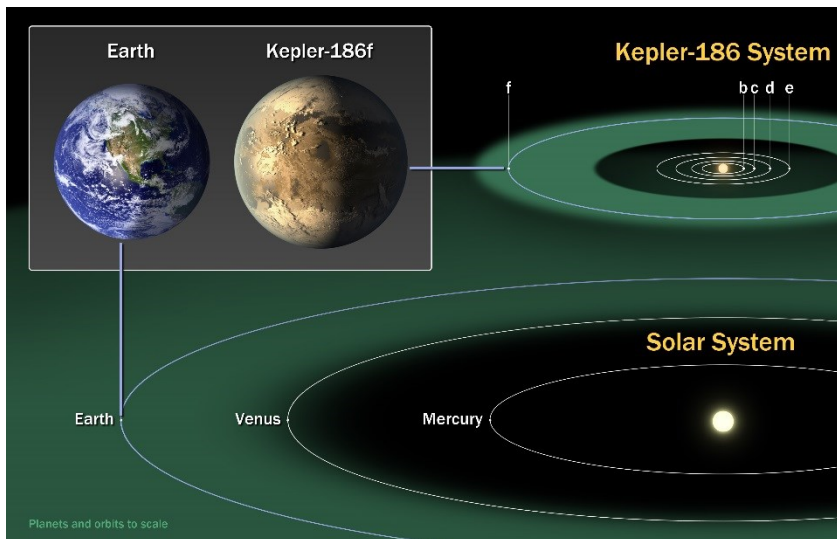
E. Quintana: Constraints on Planet Formation from KEPLER

Solar system:

- In situ formation, disk model (Minimum Mass Solar Nebula)

Kepler's multiplanet systems:

- Many super-Earths and sub-Neptunes (in situ: needs massive disk)
- No MMSN (different density profiles)



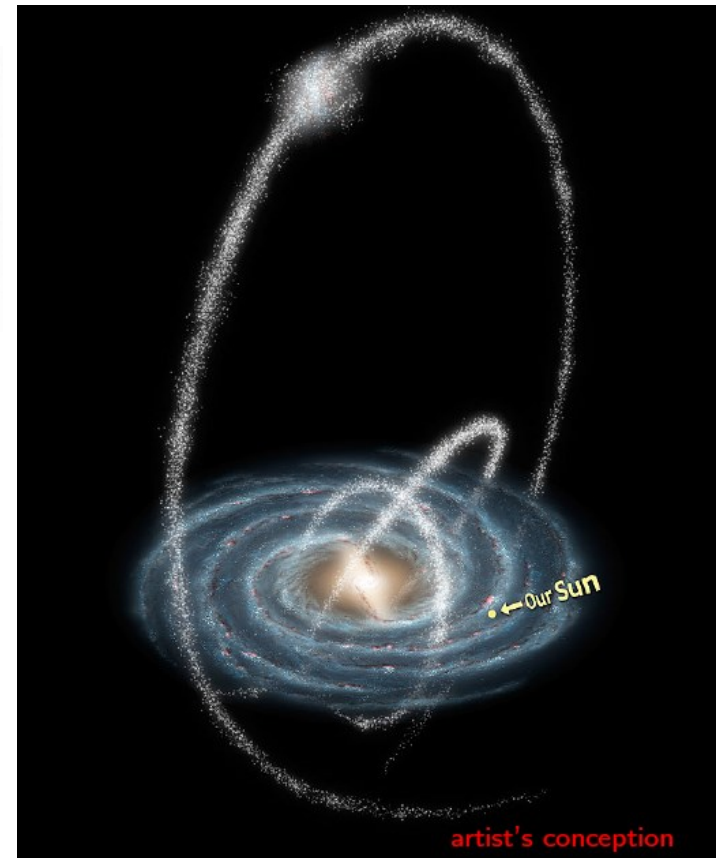
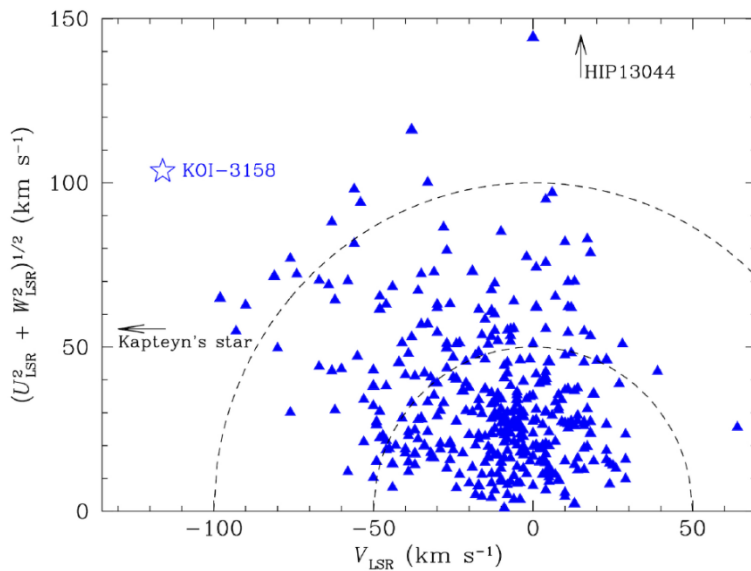
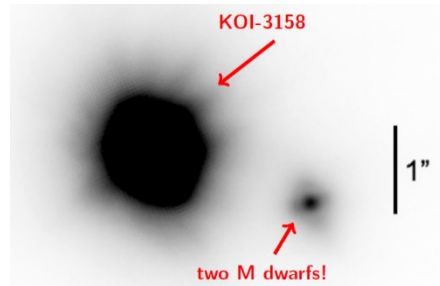
T. Campante: Extremely compact system KOI-3158

Host star K0V has 1/3 solar [Fe/H] and overabundance of Ti, Si

Very large galactic velocities

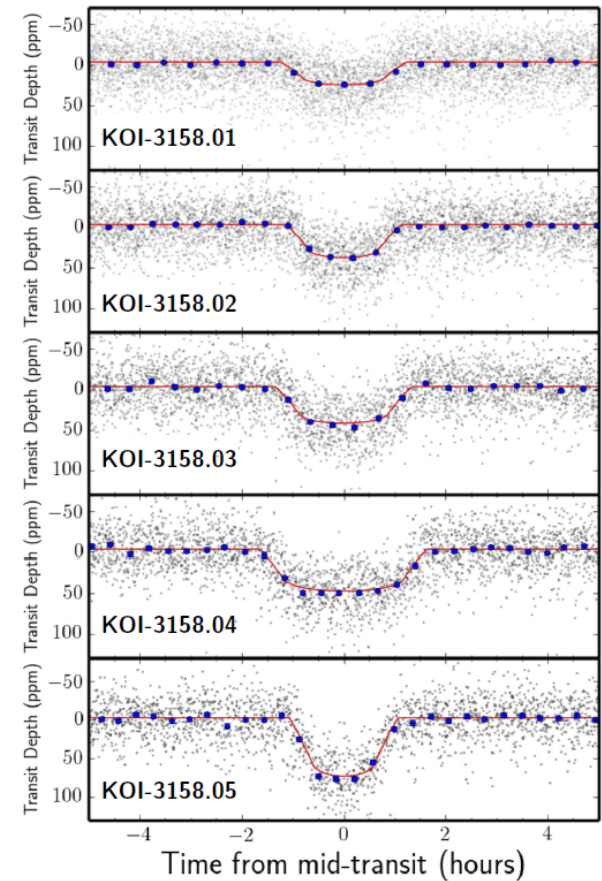
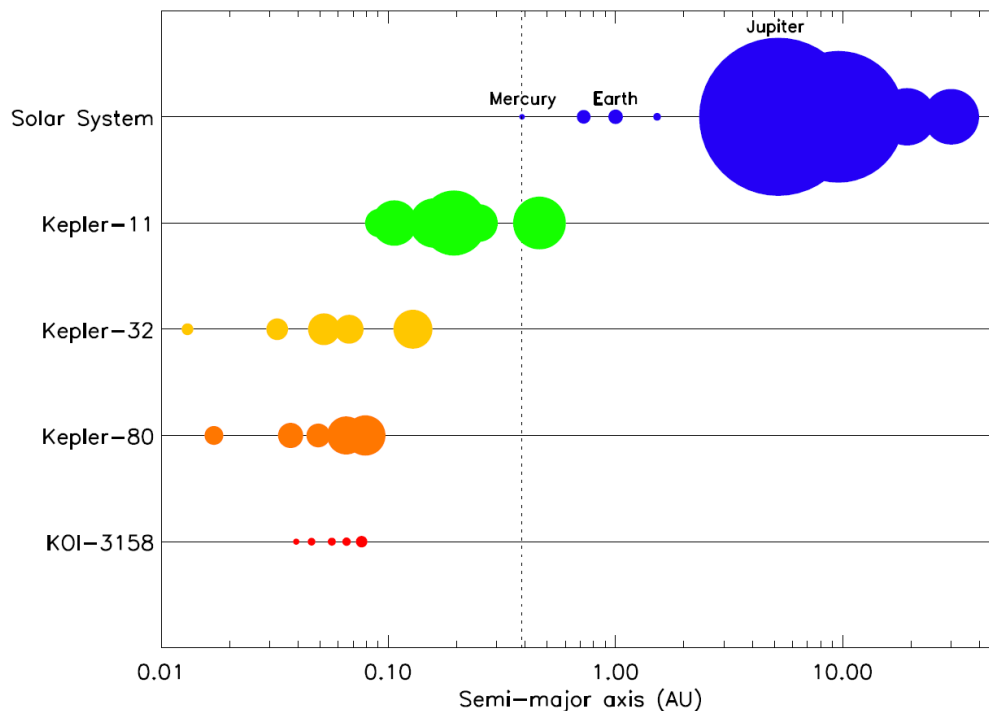
Hierarchical triple ★

Age: **11.2 Gyr!**



T. Campante: Extremely compact system KOI-3158

- 5 planets, MCMC modelling
- All under 0.08 AU and 10 day P
- Strong orbital resonances (5:4 and 4:3)



G. Ricker: TESS

Transiting Exoplanet Survey Satellite (arXiv:1406.0151)

Collaboration of MIT (PI, payload), NASA (mission, pipeline) ... Others

Goal: discover transiting earths and super-earths @ nearby bright stars

F, G, K dwarf of +4 to +12 mag, M dwarfs < 60 pc

“All sky” (400 × Kepler field) in 2 years:

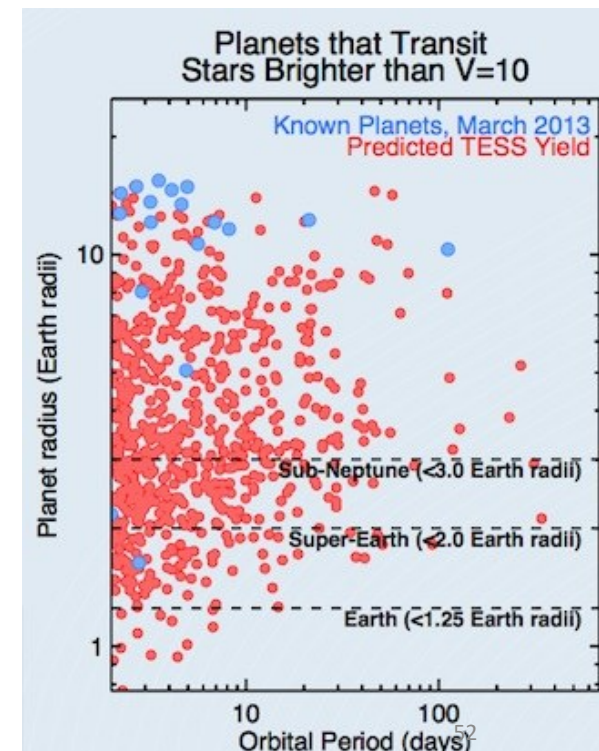
- <2 min cadence: 200 000+ targets
- 30 min cadence: 20 million targets in full frame

Hopes to have ~ 1000 exoplanets

4 cameras with 24° × 24° FOV each

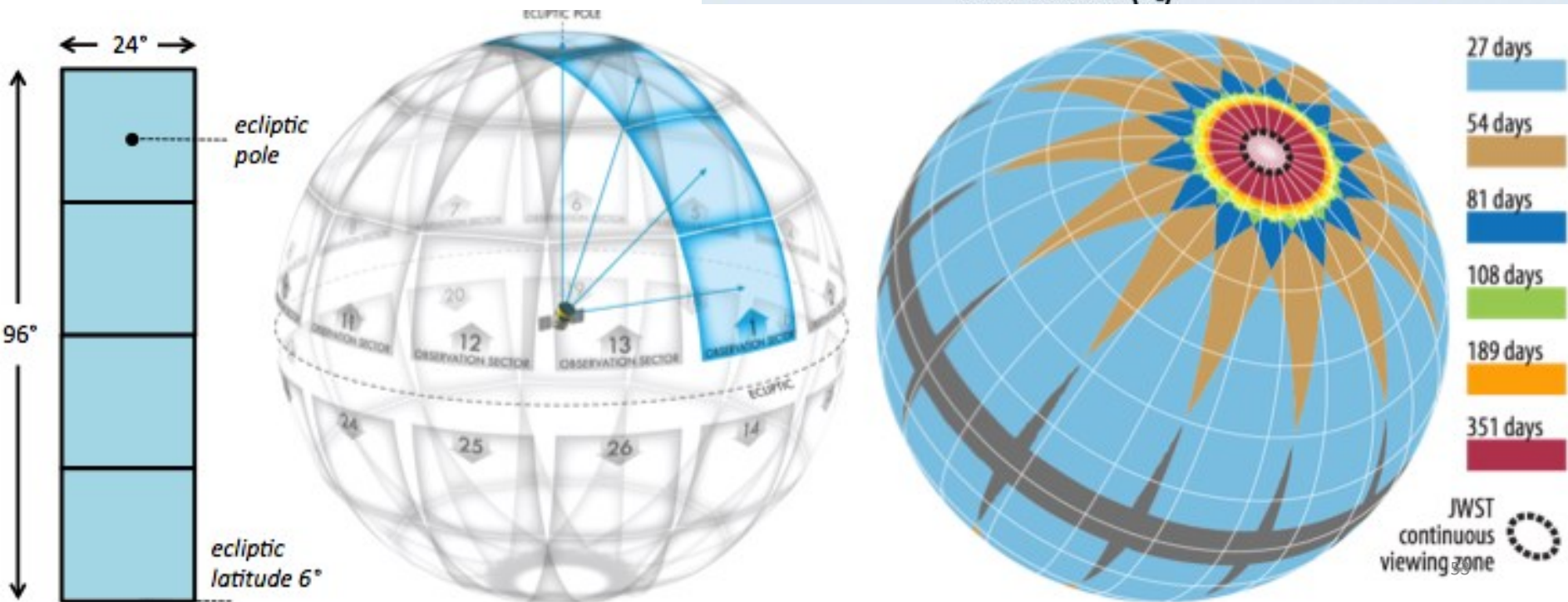
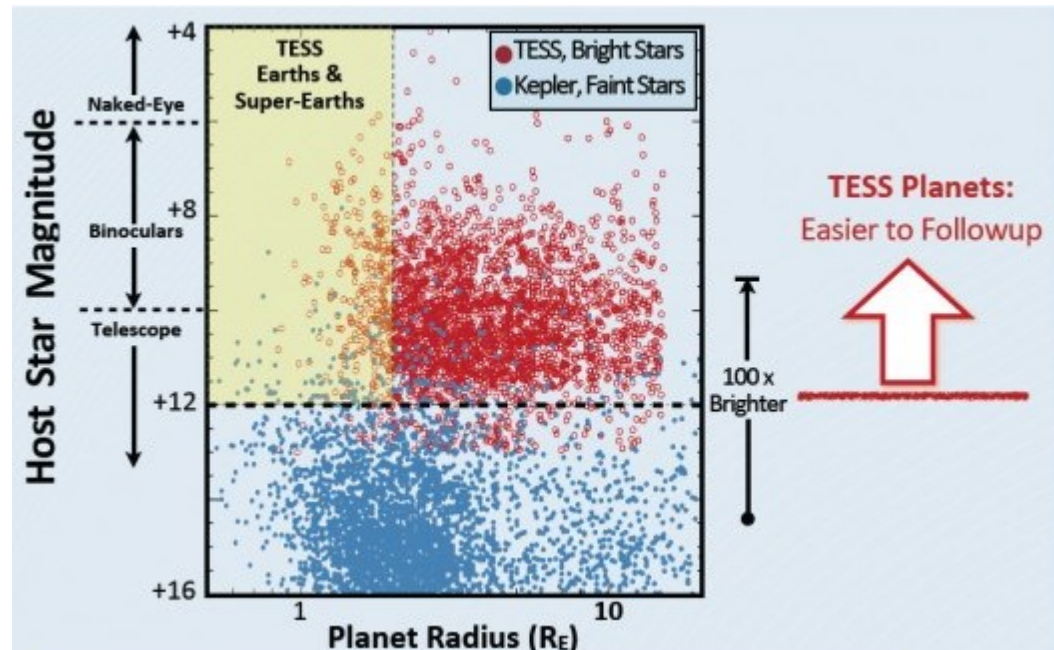
Data in MAST in 4 months after acquisition

Launch date: 2017



G. Ricker: TESS

Perigeum: $17 R_E$
 Apogeum: $59 R_E$
 $P = 13.7$ day
 Resonant with Moon 2:1
 95% of uninterrupted viewing



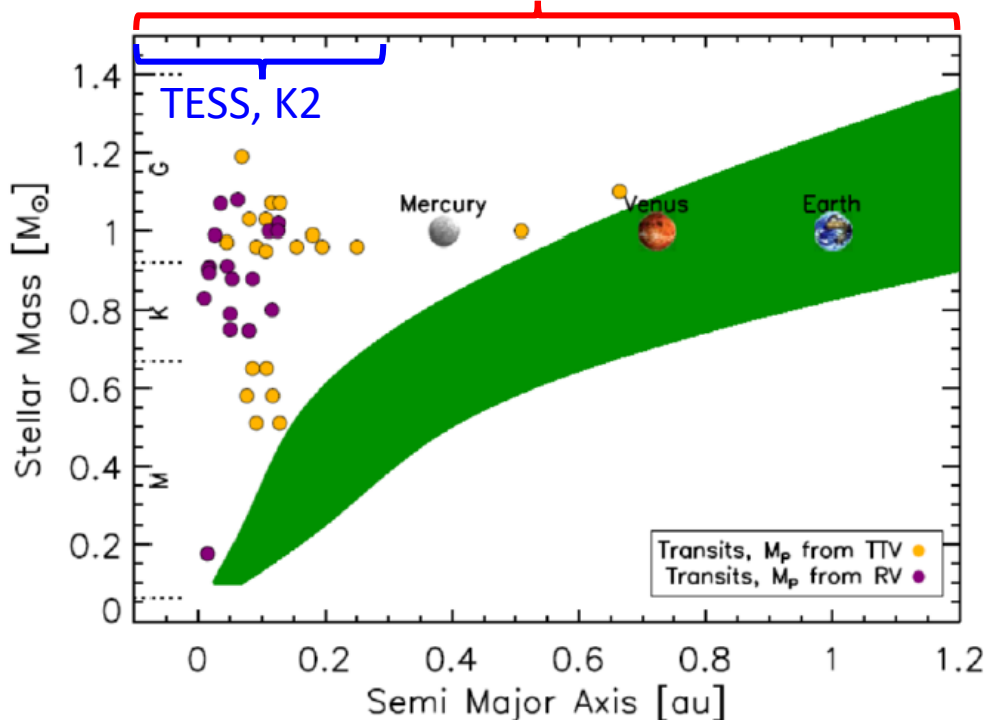
H. Rauer: Plato

PLANetary Transits and Oscillation of stars, ESA mission

New version of mission (review in March 2016), launch Q1 2024

Goals: earth-size planets with parameters ($R \sim 2\%$, $M \sim 10\%$, age $\sim 10\%$)

Fill in for longer orbital periods



Bright stars:

4-11 mag for full characterisation

13 mag for earth-size detection

16 mag for larger planet detection

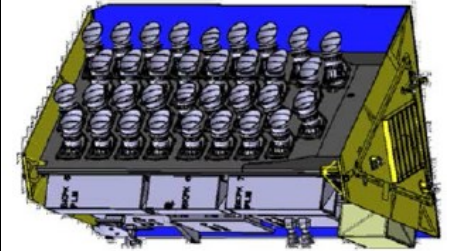
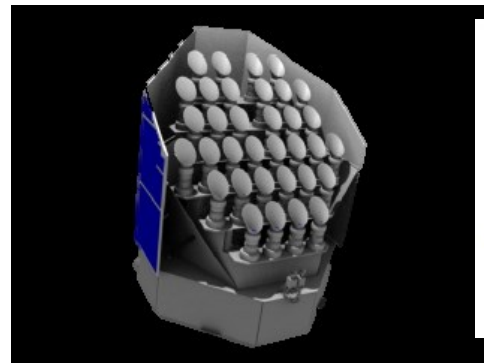
32 cameras, 25 s cadence, white light

2 cameras, 2.5 s cadence, 2 colors

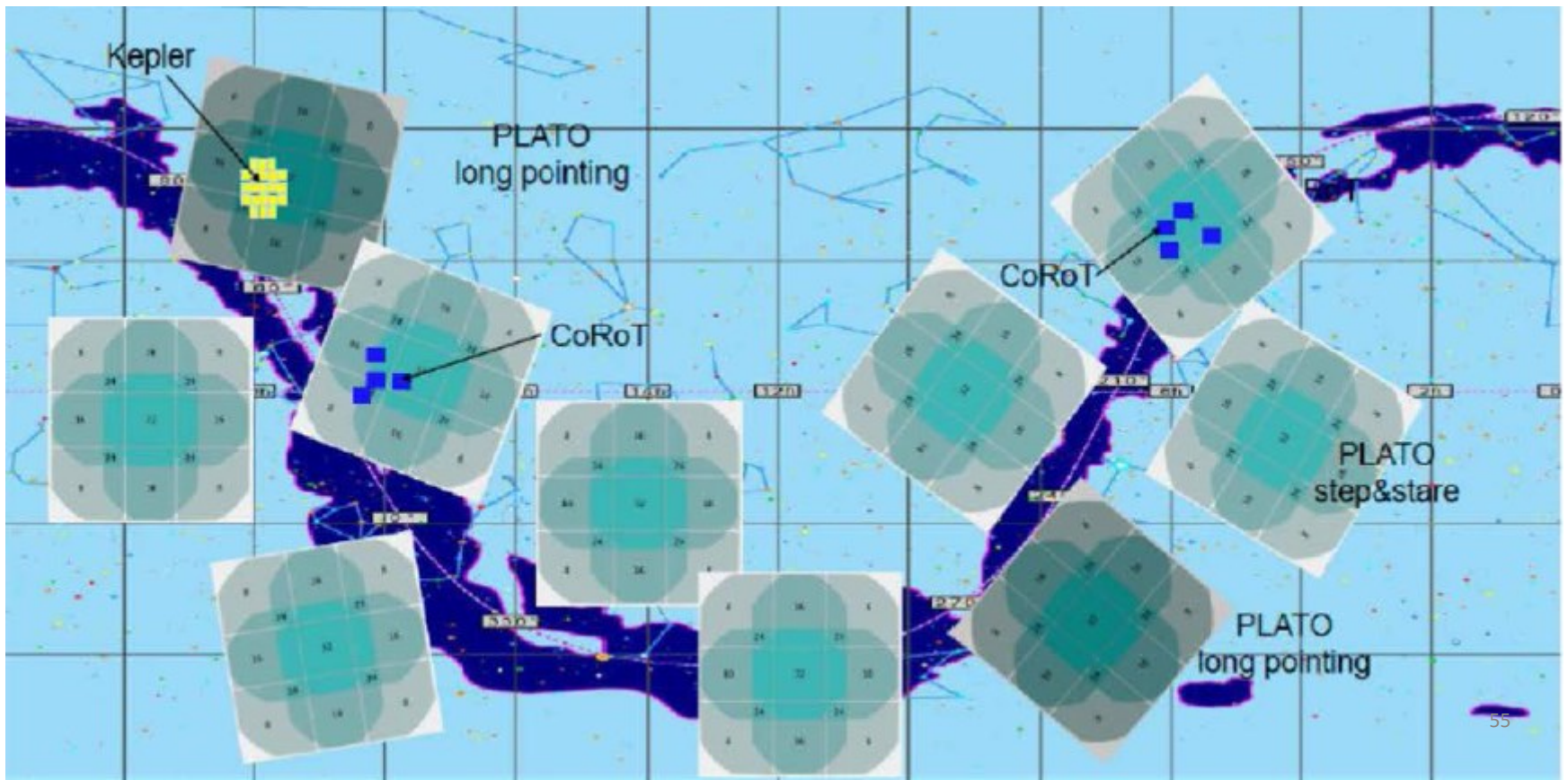
L2 orbit, mission duration: 6 years

$48.5^{\circ} \times 48.5^{\circ}$ FOV

H. Rauer: Plato



2-5 months per field, 50% sky coverage



M. Still: K-2

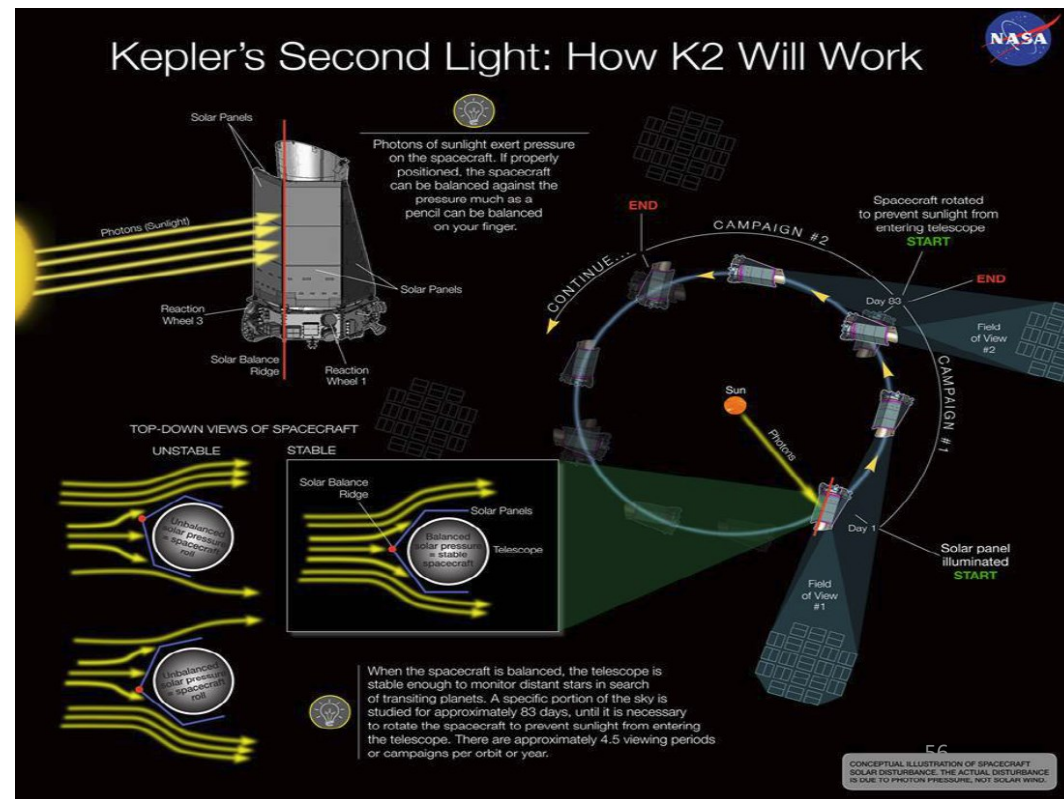
2/4 reaction wheels remain – problem with solar pressure

NASA gives budget for 2+2(optional) years /2014-2017/

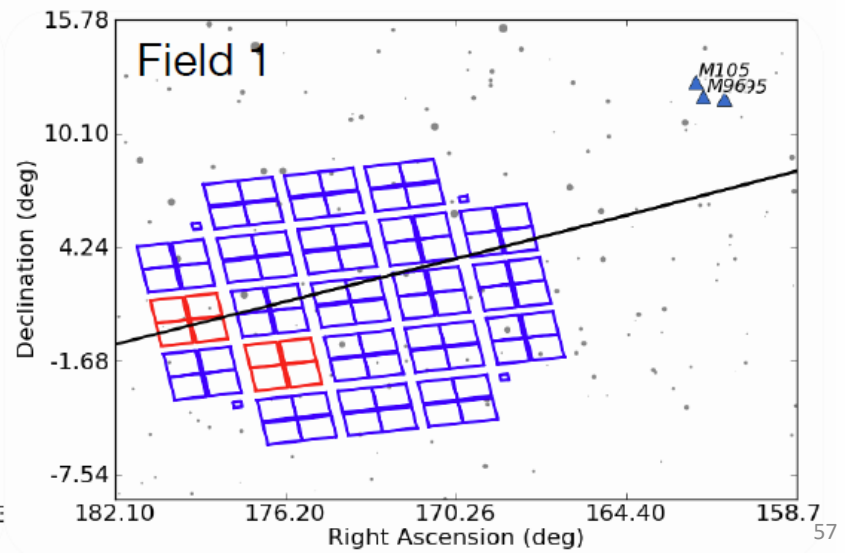
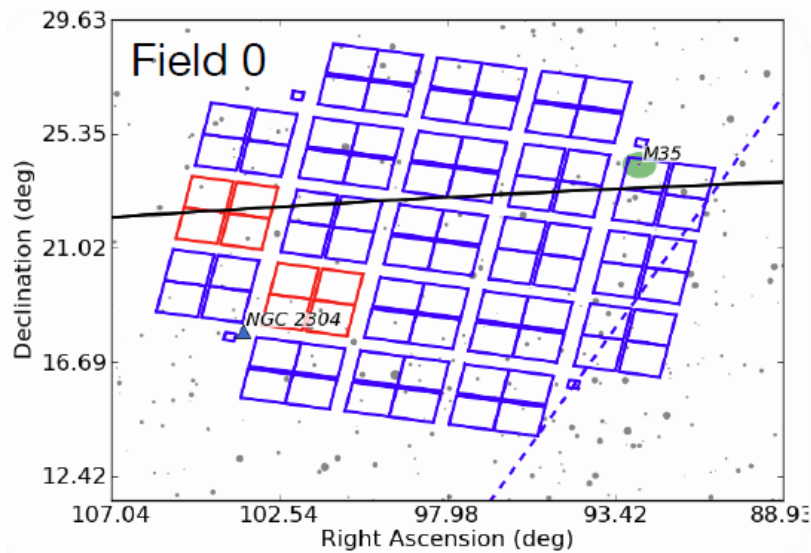
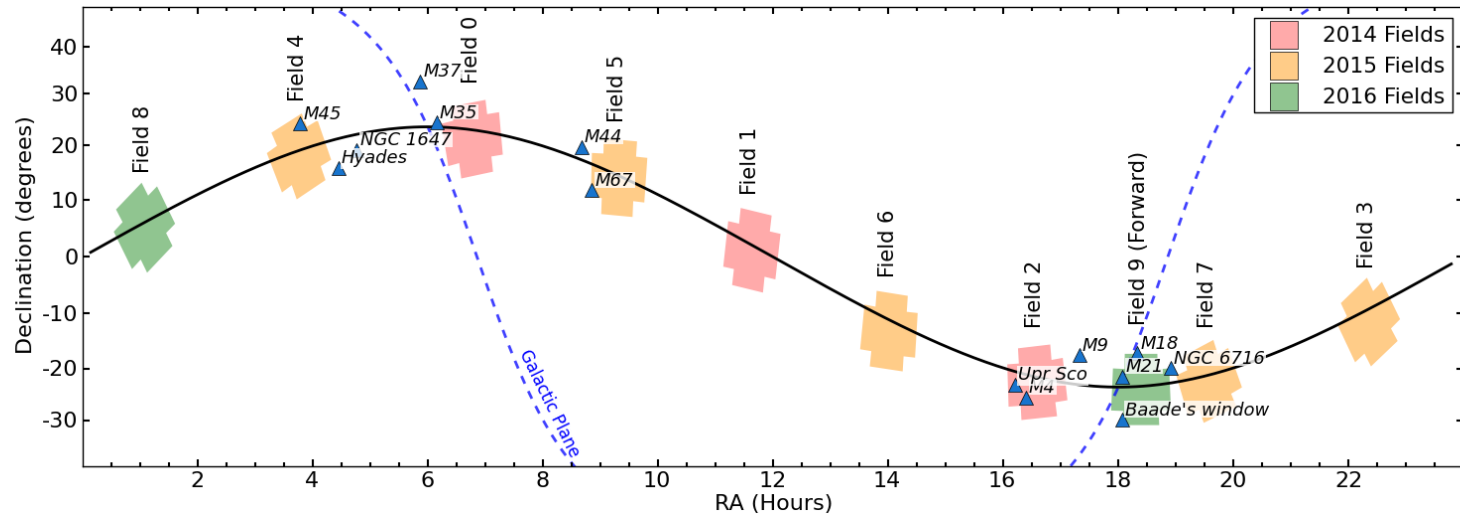
Photometric precision (100-600 ppm) 3 x worse than Kepler

New rules:

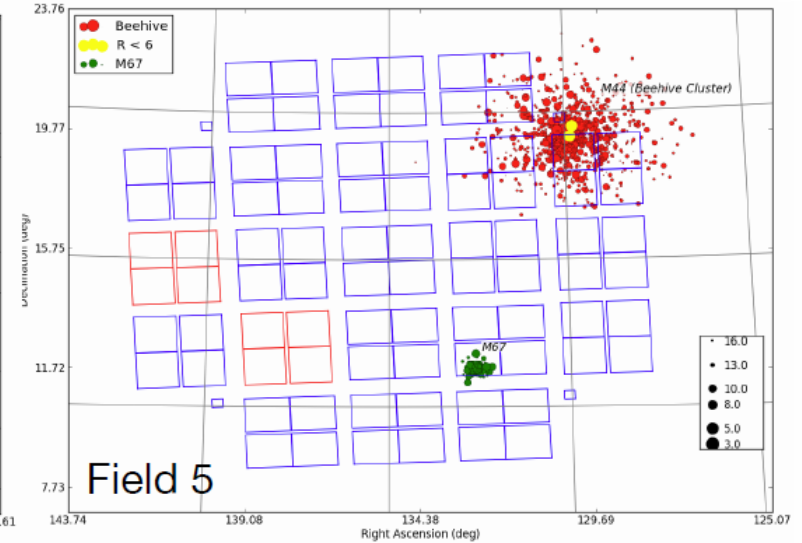
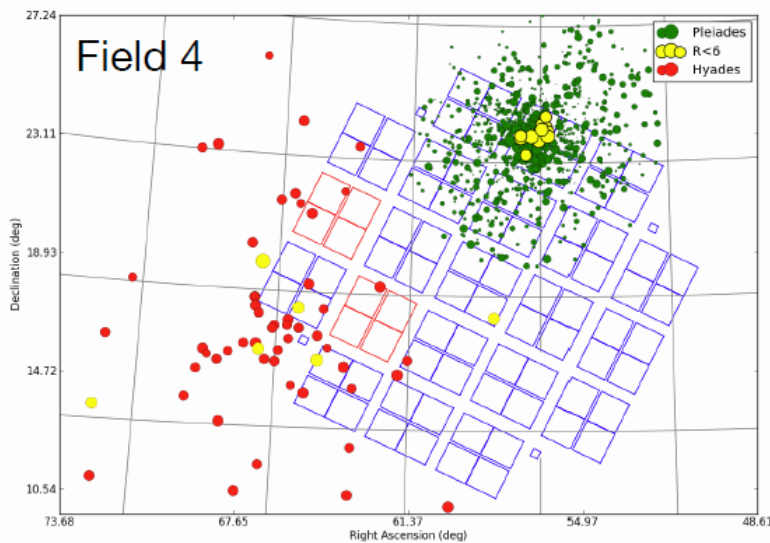
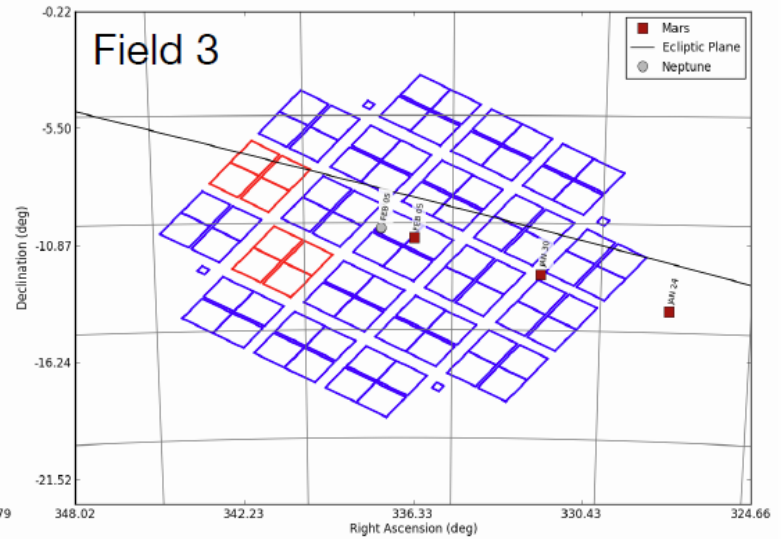
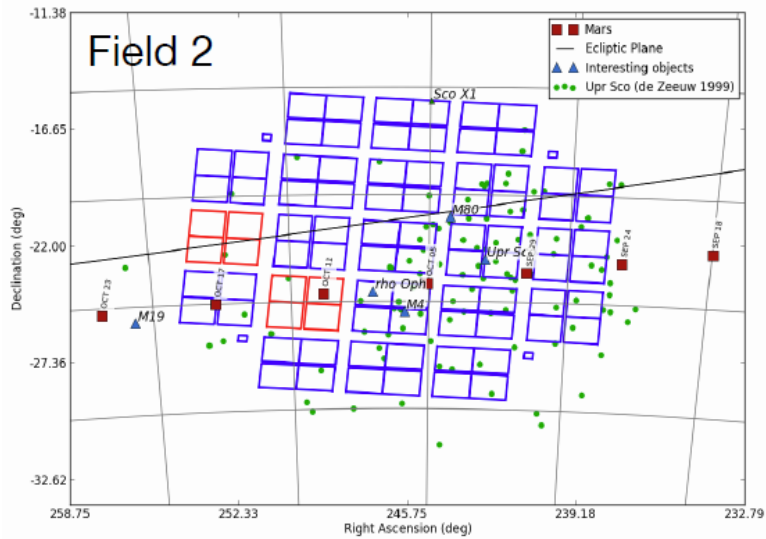
- Community defines final field locations
- Targets proposed competitively
- Program peer reviewed
- No exclusive use period



M. Still: K-2



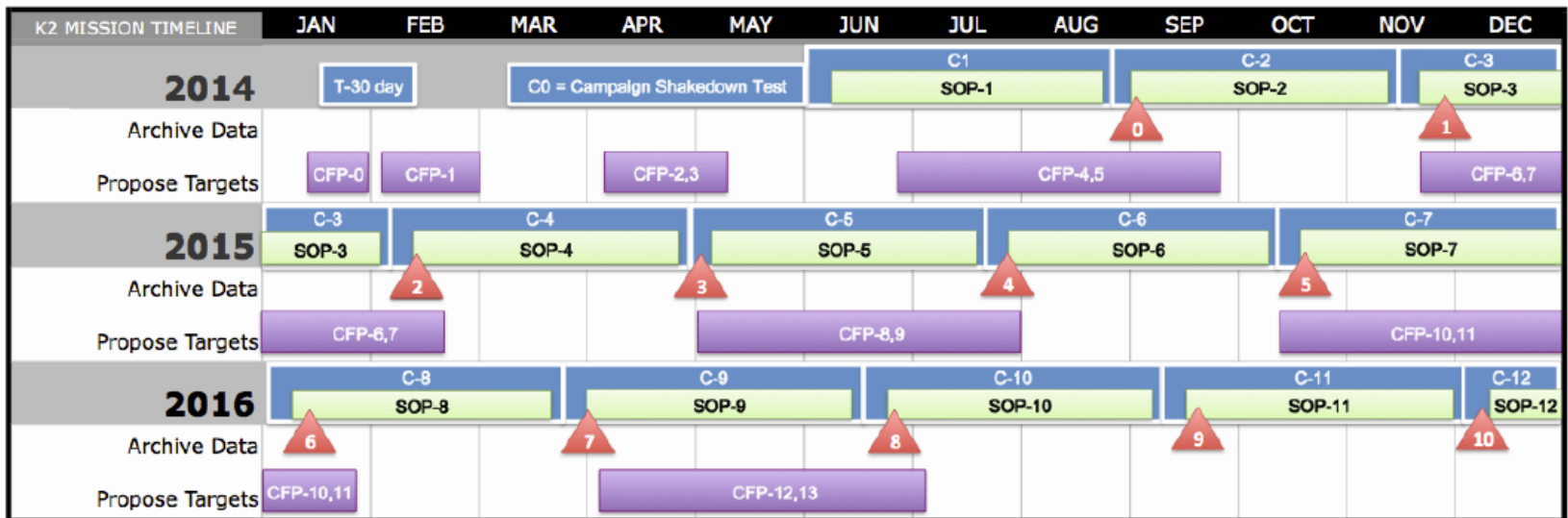
M. Still: K-2



M. Still: K-2

Science targets:

stars of different ages, young stars (Pleiades), old stars (clusters),
cool stars, bright stars,
microlensing (some fields close to galactic center),
extragalactic (SN, fields above and below the galactic plane)



T = test

C = Campaign

SOP = Science Observation Period

CFP = Call For Proposals (community target selection)



Campaign Data to Archive

C. Damiani: Star-planet interactions

Interactions:

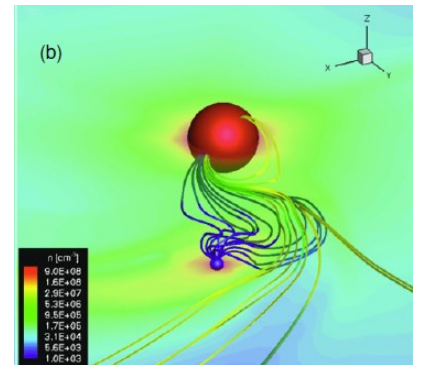
- Irradiation – evaporation (WASP-12b obscured)

(Haswell et al., 2012: *ApJ*, **760**, 79)



- Magnetic fields – (MHD simulations of HD189733b)

(Cohen et al., 2011: *ApJ*, **733**, 67)



- Gravitation – tidal torque $\propto a^{-6}$

Close-in giant planets cannot form in situ

C. Damiani: Star-planet interactions

(Barker & Ogilvie, 2009: *MNRAS*, **395**, 2268)

Tidal circularization time (for co-planar orbit)

$$\tau_e \approx 16.8 \text{ Myr} \left(\frac{Q'_\star}{10^6} \right) \left(\frac{m_\star}{M_\odot} \right)^{\frac{8}{3}} \left(\frac{M_J}{m_p} \right) \left(\frac{R_\odot}{R_\star} \right)^5 \left(\frac{P_{\text{orb}}}{1 \text{ d}} \right)^{\frac{13}{3}} \\ \times \left[\left(f_1(e) - \frac{11}{18} \frac{P_{\text{orb}}}{P_\star} f_2(e) \right) + \frac{Q'_p}{Q'_\star} \left(\frac{m_\star}{m_p} \right)^2 \left(\frac{R_p}{R_\star} \right)^5 \left(f_1(e) - \frac{11}{18} f_2(e) \right) \right]^{-1}$$

$$\tau_e \approx 4 \text{ Myr, for } e = 0.4 \text{ and } P_{\text{orb}} = 3 \text{ d}$$

Tidal alignment time (for circular orbit and small inclination)

$$\tau_i \approx 70 \text{ Myr} \left(\frac{Q'_\star}{10^6} \right) \left(\frac{m_\star}{M_\odot} \right) \left(\frac{M_J}{m_p} \right)^2 \left(\frac{R_\odot}{R_\star} \right)^3 \left(\frac{P_{\text{orb}}}{1 \text{ d}} \right)^4 \frac{12.5 \text{ d}}{P_\star} \left[1 - \frac{P_{\text{orb}}}{2P_\star} \left(1 - \frac{I\Omega}{h\mu} \right) \right]^{-1}$$

$$\tau_i \approx 6 \text{ Gyr, for } P_{\text{orb}} = 3 \text{ d and } P_\star = 12.5 \text{ d}$$

Tidal inspiral time (neglecting tides in the planet and for circular and co-planar orbit)

$$\tau_a \approx 12.0 \text{ Myr} \left(\frac{Q'_\star}{10^6} \right) \left(\frac{m_\star}{M_\odot} \right) \left(\frac{M_J}{m_p} \right) \left(\frac{P_{\text{orb}}}{1 \text{ d}} \right)^{\frac{13}{3}} \left(1 - \frac{P_{\text{orb}}}{P_\star} \right)^{-1}$$

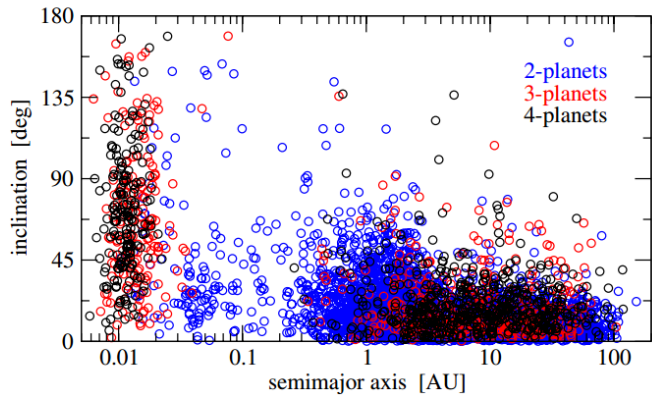
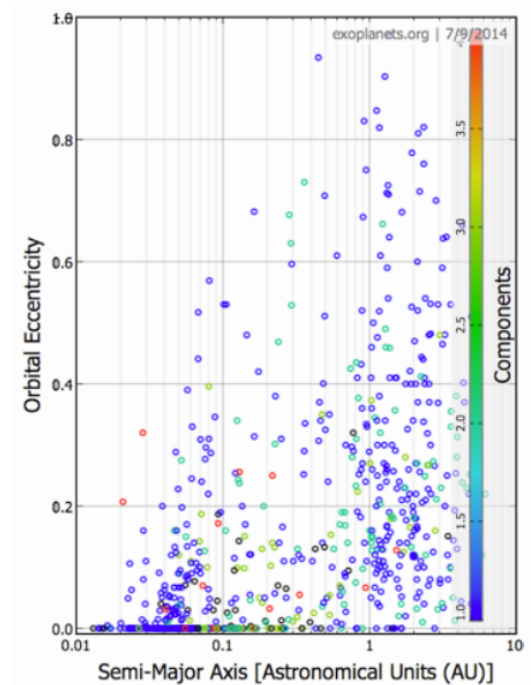
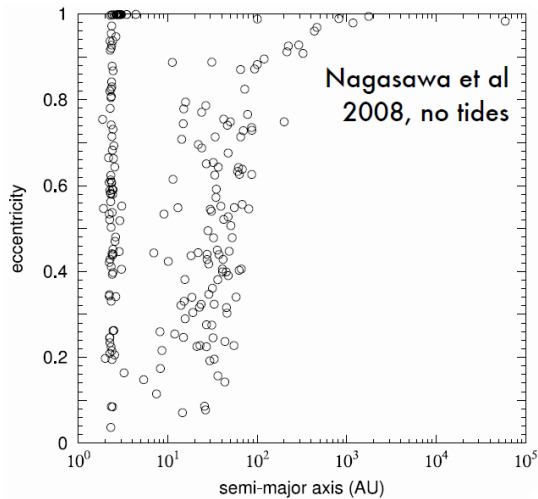
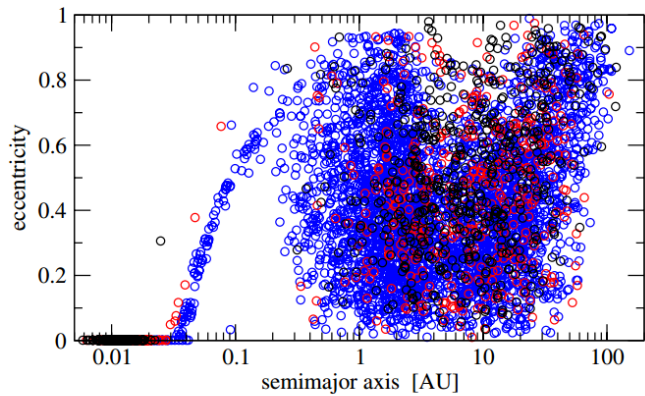
$$\tau_a \approx 2 \text{ Gyr, for } P_{\text{orb}} = 3 \text{ d and } P_\star = 12.5 \text{ d}$$

C. Damiani: Star-planet interactions

Planet-scattering (with tides)

(without tides)

(observed)



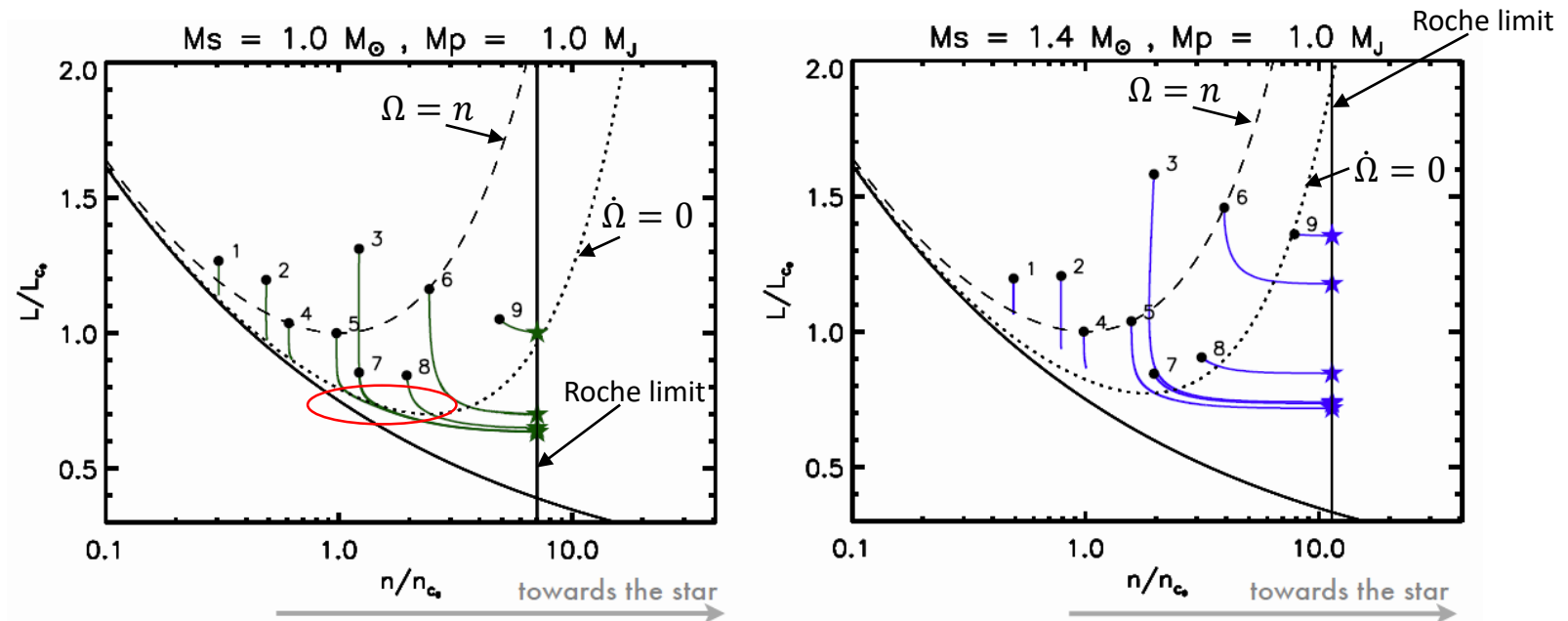
(Nagasawa et al., 2008:
IAUS, 249, 279)

(Beaugé & Nesvorný, 2012: *ApJ*, 751, 119)

C. Damiani: Star-planet interactions

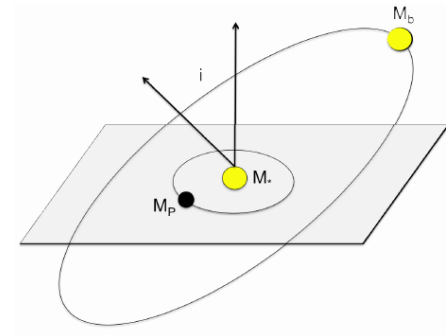
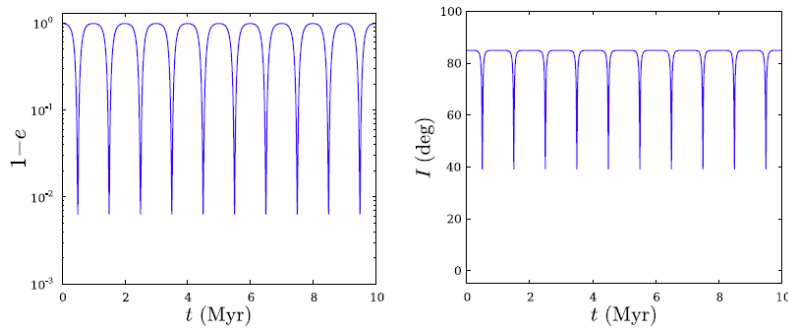
G stars loose \vec{L} from their magnetized wind, F stars less so

The dynamical evolution of orbital elements is driven by the resultant of the wind torque and the tidal torque



K. Andersson: Evolution of stellar spin

Kozai mechanism:



+ corrections:

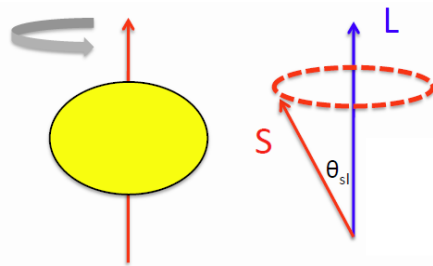
GR periastron precession, tides, oblateness, tidal dissipation in planet

→ orbital decay

What happens to the stellar spin?

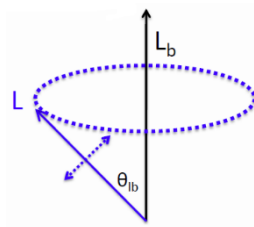
K. Andersson: Evolution of stellar spin

Tide from planet on oblate star spin:

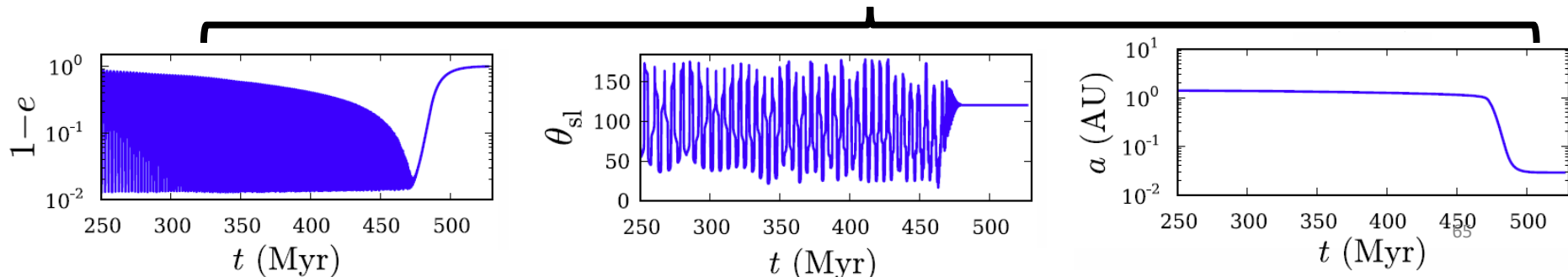
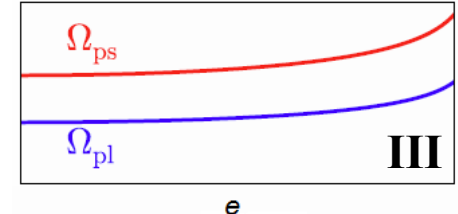
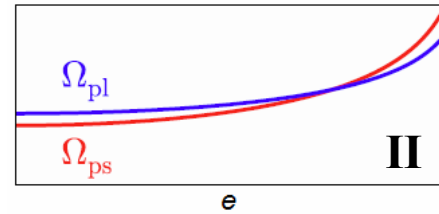
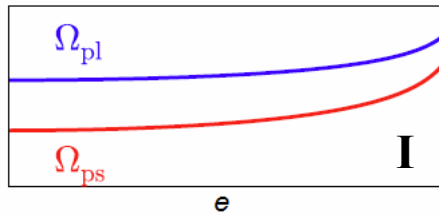
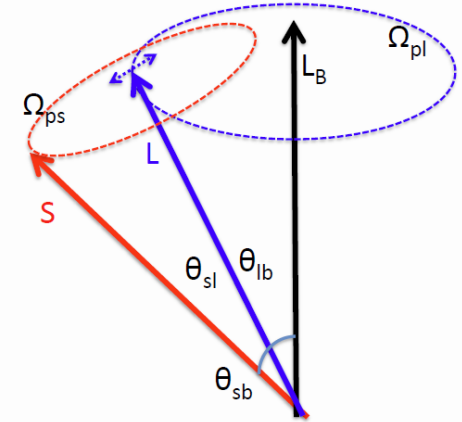


$$\Omega_{ps} \sim (1 - e^2)^{-3/2}$$

Planet orbit precession and nutation:



$$\Omega_{pl} \sim (1 - e^2)^{-1}$$



V. Silva Aguirre: Astroseismology for exoplanet characterization

From LCs (assumes circular orbit):

$$\Delta F = \left(\frac{R_P}{R_{\star}}\right)^2 \langle \rho_{\star} \rangle \approx \frac{3\pi}{GP^2} \left(\frac{a}{R_{\star}}\right)^3 \quad (\text{Seager \& Mallén Ornelas, 2003: } \textit{ApJ}, \mathbf{585}, 1038)$$

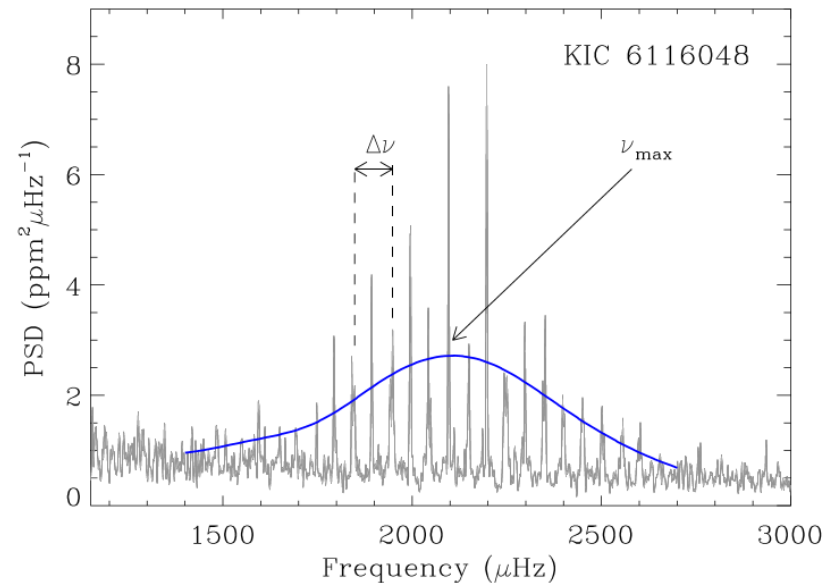
From asteroseismology:

$$\frac{M}{M_{\odot}} \cong \left(\frac{v_{\max}}{v_{\max,\odot}}\right)^3 \left(\frac{\Delta\nu}{\Delta\nu_{\odot}}\right)^{-4} \left(\frac{T_{\text{eff}}}{T_{\text{eff},\odot}}\right)^{3/2};$$

$$\frac{R}{R_{\odot}} \cong \left(\frac{v_{\max}}{v_{\max,\odot}}\right) \left(\frac{\Delta\nu}{\Delta\nu_{\odot}}\right)^{-2} \left(\frac{T_{\text{eff}}}{T_{\text{eff},\odot}}\right)^{1/2};$$

$$\rho_{\star} = \frac{3M}{4\pi R^3}$$

(Chaplin et al., 2011: *Science*, **322**, 213)



(Chaplin et al., 2014: *ApJS*, **210**, 1)

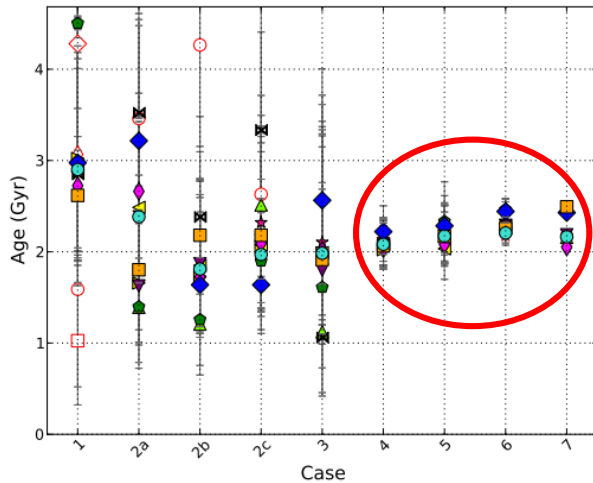
V. Silva Aguirre: Astroseismology for exoplanet characterization

Compare densities – some consideration of e

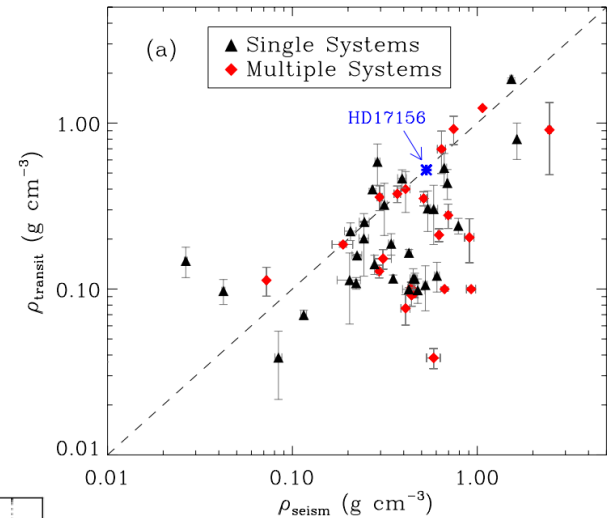
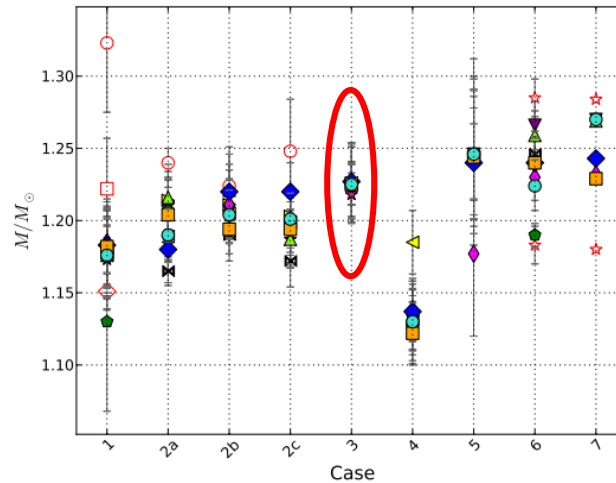
$$\frac{\rho_{\text{seism}}}{\rho_{\text{transit}}} = \frac{(1 - e^2)^{3/2}}{(1 + e \sin \omega)^3}$$

(Van Eylen, et al., 2014: *ApJ*, **782**, 14)

Age & M – best errors from seismology



(Lebreton & Goupil, 2014: *A&A*, **569**, 21)



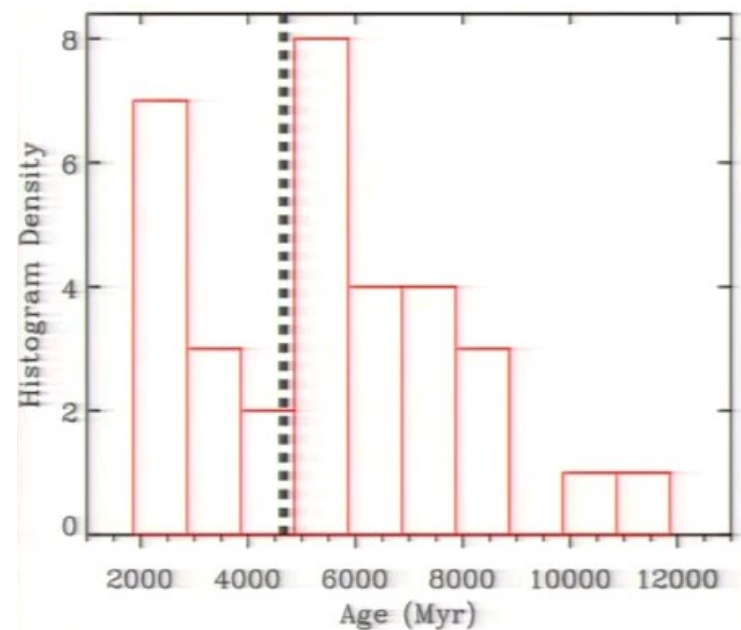
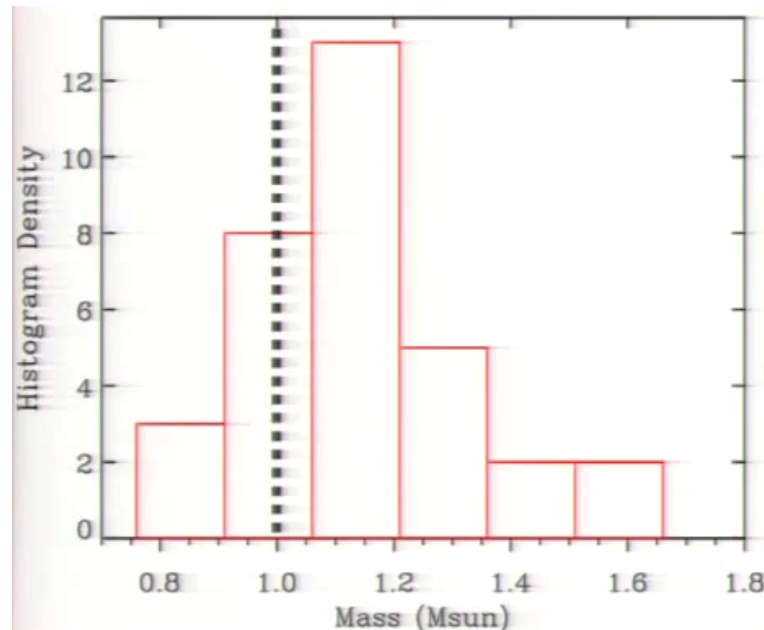
(Huber et al., 2013: *ApJ*, **767**, 127)

1 = only T_{eff} , $[\text{Fe}/\text{H}]$, L
>3 = seism. freq. analysis

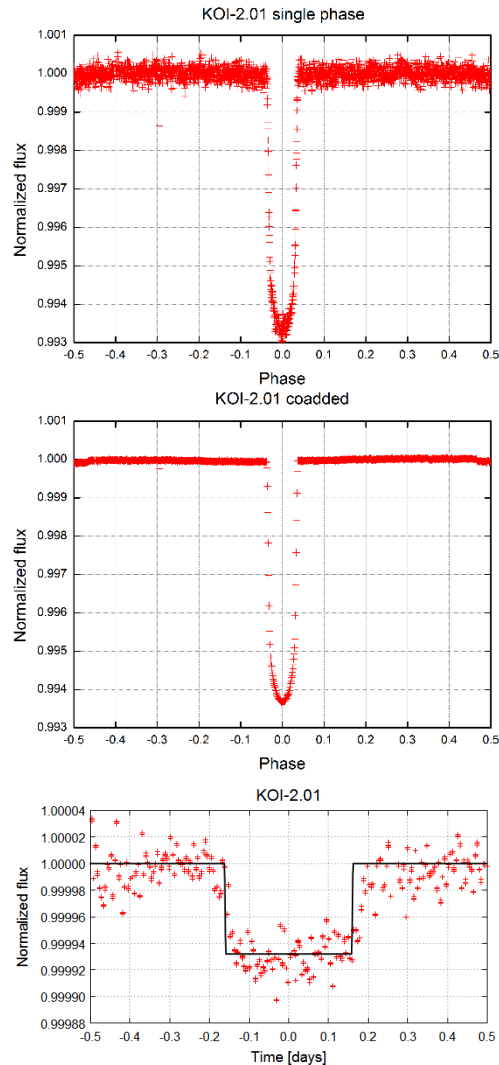
V. Silva Aguirre: Astroseismology for exoplanet characterization

Project Kages:

- 33 KOIs (up to 500 pc) so far, with ν , M , age determined
- Errors: $R \sim 3\%$, $M \sim 8\%$, age $\sim 15\%$
- Also KOI-3158 (oldest known host of terrestrial exoplanets)



My presentation



Modelling secondary eclipses of *KEPLER* exoplanets

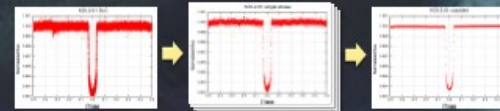
Lubomír Hambálek¹ (lhambalek@ta3.sk)

¹ Astronomical Institute of Slovak Academy of Sciences, Tatranská Lomnica, Slovakia

Abstract: The occultation of the transiting exoplanet by its parent star will manifest on the light-curve as a shallow secondary minimum. The precise photometry obtained by the *KEPLER* spacecraft (and other similar space telescopes) theoretically allows us to distinguish the secondary minimum. In their paper, Coughlin & López-Morales (2012, *AJ*, 143, 39) tried to select *KEPLER* candidates with potentially deep secondary minima. We have selected several candidates with the deepest secondary eclipses. By combining many short-cadence light-curves we have produced a smoother light-curve with a stronger signal and made the secondary minima more distinct. This allowed us to measure the depth of primary and secondary minimum and to determine stellar and planetary radii.

Our motivation was the paper by Coughlin & López-Morales (2012) who tried a systematic approach. We used their results to select potential candidates with sufficient potential depth of secondary eclipses. Objects with high luminosity ratio (L_p/L_s) and a high significance of the detection of the secondary minimum (σ_{II}) were selected. KOI-1541.01 and KOI-1543.01 both with highest L_p/L_s show flux variations due to the presence of photospheric spots, thus we decided not to impose additional possible trends to the light-curve by an irregular de-trending. To compare our approach to the existing data we have selected systems KOI-2.01 and KOI-13.01 with previously identified secondary minima. Additional objects KOI-10.01, KOI-254.01 were investigated for presence of the secondary minimum.

We have used publicly available data from quarters Q0-Q16 from the Mikulski Archive for Space Telescopes (MAST). All light-curves are plotted with fluxes processed via an updated PDC pipeline and normalized. To keep better time resolution we limited the selection only for short-cadence (58.85 s) light-curves. We have applied a running linear fit with anchor points around orbital phases $\phi=0.25$ and $\phi=0.75$ to de-trend the raw data. Additionally, we have corrected the measured flux of KOI-13.01 by $\sim 45\%$ (Szabó et al., 2011) of total maximum flux to remove the parasitic light of the second stellar component. We have modelled the depth of the secondary minimum with respect to the reflection and ellipsoidal variations (Mazeh et al., 2012).



Co-addition process illustrated at the case of KOI-2.01. Note the decrease of noise in data.

We divided the time series into separate epochs. Then we have selected only phased light-curves with time series longer than 0.5P which contained data around the planetary occultation at $\phi=0.5$. We have then used a spline interpolation based on the Hermite polynomials (Press et al., 1992) to co-add the particular phased light-curves. For KOI-2.01 and KOI-13.01 we have added together 148 and 93 full and/or partial exoplanet orbits, respectively. The noise in normalized flux dropped down to 20-50% of previous noise value and we have measured the depths of primary Δ_I and secondary minima Δ_{II} (see the table).

We have used an simplex algorithm to minimize analytical expressions of the transit geometry (Mandel & Agol, 2002) to fit primary and secondary minima for both planetary candidates. Initial values of the ratio of planetary and stellar radii (R_p/R_s), the ratio of the stellar radius to the separation (R_s/a) and the time of primary minimum (T_0) were adopted from the table of *KEPLER* candidates at MAST. Initial inclination (i) was adopted from Coughlin & López-Morales (2012). Quadratic limb darkening coefficients (u_1, u_2) were interpolated from Sing (2010).

	KOI-2.01	KOI-13.01	KOI-10.01	KOI-254.01			
i [deg]	83.88	83.92	81.00	79.79	84.26	87.19	87.00
Δ_I [ppm]	6297	6716	7831	4644	9463	9390	1
Δ_{II} [ppm]	88	130	157	120	3	-	-
R_p [R_J]	0.100	0.104	0.204	0.165	0.148	0.142	4
R_s [R_S]	1.3361	1.336	2.4541	2.454	1.561	1.56	5
Δ_{II}/Δ_I	0.011	0.019	0.020	0.026	-	-	-
R_p/R_s	0.075	0.078	0.083	0.067	0.095	0.091	0.189
u_1	0.3135	0.3532	0.2496	0.2526	-	-	-
u_2	0.3102	0.2876	0.2910	0.2932	-	-	-

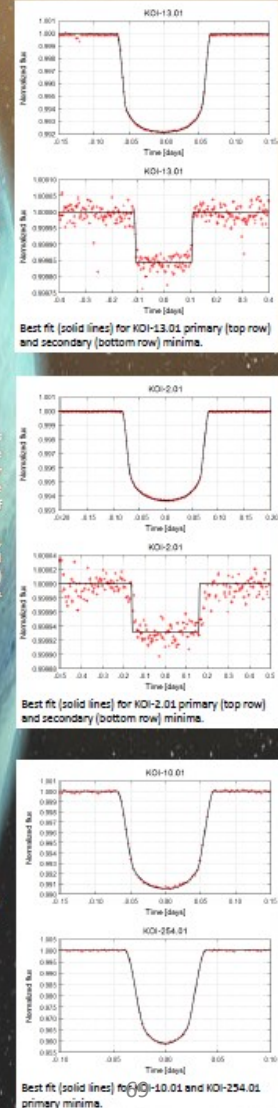
Results from modelling primary and secondary minima. Bold face values represent results of this work, previous results are cited for comparison. Values marked with "1" are fixed. Sources: 1) Borucki et al., 2010, 2) Coughlin & López-Morales, 2012, 3) Szabó et al., 2011, 4) Jenkins et al., 2010 and 5) Johnson et al., 2012.

Acknowledgments:

This research has been funded by grants VEGA 2/0143/14 and APVV-0158-11. LH acknowledges the stipend of the Štefan Schwarz fund of the Slovak Academy of Sciences. This paper includes data collected by the Kepler mission. Funding for the Kepler mission is provided by the NASA Science Mission Directorate.

References:

- Borucki, W.J. et al., 2011, *AJ*, 736, 19
- Coughlin, J.L. & López-Morales, M., 2012, *AJ*, 143, 39
- Jenkins, J.M. et al., 2010, *AJ*, 724, 1108
- Johnson, J.A. et al., 2012, *AJ*, 143, 111
- Mandel, K. & Agol, E., 2002, *AJ*, 580L, 171
- Mazeh, T. et al., 2012, *A&A*, 541, 56
- Press, W.H. et al., 1992, *Numerical Recipes*, Cambridge University Press
- Sing, D.K., 2010, *A&A*, 510, A21
- Szabó, Gy.M., Szabó, R., Benkő, J.M. et al., 2011, *AJ*, 736L, 4



Instead of a summary



Instead of a summary



Jaymie Matthews



Instead of a summary

The collage features several handwritten notes and diagrams:

- BRANDON TINGLEY AARHUS UNIVERSITY STELLAR ASTROPHYSICS CENTER**: A blue note at the top center.
- IN GAIA PHOTOMETRY**: A note on the top left discussing the GAIA mission's photometry and the challenges of detecting exoplanets.
- GAIA SCANNING LAW**: A note with a diagram showing the scanning law, which plots the number of stars as a function of distance from Earth.
- ASTROMETRIC PLANETS**: A note in the center discussing the discovery of exoplanets with full orbital solutions, including periods and inclinations.
- THREE TYPES OF PLANETS WE CAN GO AFTER**: A note on the middle left listing: 1) HOT JUPITERS, 2) TERRESTRIAL HABITABLE ZONE PLANETS ORBITING IN DWARF STARS, and 3) ASTROMETRIC PLANETS WITH HIGH PROBABILITY OF TRANSITING.
- LOOK! KITTENS!**: A note on the middle left featuring a photo of two kittens.
- HOT JUPITERS**: A note on the bottom left discussing the discovery of hot Jupiters and their characteristics.
- THEORY DETECTION ALGORITHM**: A note on the bottom left describing an algorithm for detecting exoplanets.
- GAIA SCANNING LAW**: A note with a diagram showing the scanning law, which plots the number of stars as a function of distance from Earth.
- HOW WILL IT ACCOMPLISH THIS?**: A note on the top right listing various methods used by GAIA, such as astrometry, photometry, and spectroscopy.
- TERRESTRIAL HABITABLE ZONE PLANETS ORBITING IN DWARF STARS**: A note on the middle right discussing the discovery of exoplanets in the habitable zone of dwarf stars.
- COMFUSED? GOOD!**: A note on the middle right featuring a drawing of a bear and discussing the challenges of exoplanet discovery.
- I'M SORRY, DAVE**: A note on the bottom right featuring a drawing of a bear and discussing the challenges of exoplanet discovery.
- ALGORITHM**: A note on the bottom right featuring a drawing of a bear and discussing the challenges of exoplanet discovery.
- GAIA**: A logo at the bottom right.

Instead of a summary

2014

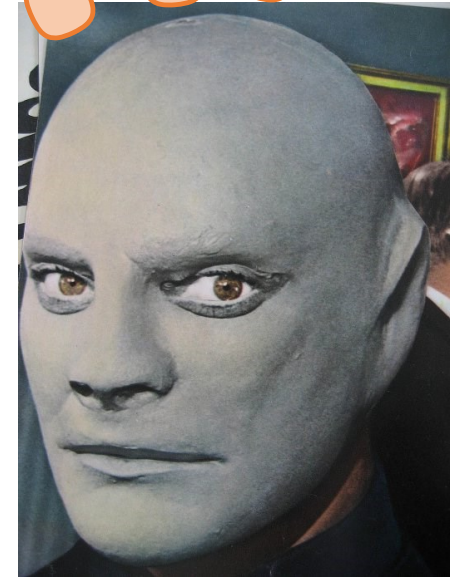


Malcolm Fridlund

1967



Fantomas



Thank you
for your attention!



July 6 – 11, 2014 – Toulouse, FRANCE